



RESEARCH MEMORANDUM

EFFECTIVENESS OF VARIOUS PROTECTIVE COVERINGS ON
MAGNESIUM FINS AT MACH NUMBER 2.0 AND
STAGNATION TEMPERATURES UP
TO 3,600° R

By William M. Bland, Jr.

Langley Aeronautical Laboratory
Langley Field, Va.

NATIONAL ADVISORY COMMITTEE
FOR AERONAUTICS
WASHINGTON

January 9, 1958

NATIONAL ADVISORY COMMITTEE FOR AERONAUTICS

RESEARCH MEMORANDUM

EFFECTIVENESS OF VARIOUS PROTECTIVE COVERINGS ON
MAGNESIUM FINS AT MACH NUMBER 2.0 AND
STAGNATION TEMPERATURES UP
TO $3,600^{\circ}$ R

By William M. Bland, Jr.

SUMMARY

Eight thin magnesium fins, seven with the leading edges swept back 17° and one with the leading edge swept back 45° , have been tested in the preflight high-temperature jet of the Langley Pilotless Aircraft Research Station at Wallops Island, Va. This investigation was made to determine the effectiveness of various protective coverings designed to alleviate aerodynamic-heating effects and intended for application on the first stages of rocket-propelled multistage hypersonic models. Temperatures were measured at various locations throughout the fins.

Results of these tests, which were conducted at a Mach number of 2.0 for various stagnation temperatures up to $3,600^{\circ}$ R, indicated that wrapping Inconel around the fin leading edges protected the adjacent magnesium structure to the melting temperature of the Inconel covering. When the fin was subjected to less severe heat inputs for a longer time, the exposed magnesium surfaces behind the Inconel covered leading edge became vulnerable to ignition and burning. Inserting a piece of Fiberglas between the Inconel cover and the magnesium appeared to decrease materially the amount of heat transferred from the Inconel to the magnesium. Also, it was determined that increasing the protective covering at the leading edge and extending protection over the exposed magnesium surfaces made the basic magnesium fin as much as four times as durable at stagnation temperatures as high as $3,400^{\circ}$ R. Effective air gaps between the layers of material were calculated by using simple heat-balance relations.

INTRODUCTION

Problems associated with flight at supersonic and hypersonic speeds are being investigated by the Langley Pilotless Aircraft Research Division with multiple-stage rocket-propelled models. Conventional fins are being used to stabilize various model-booster combinations in the supersonic speed range where aerodynamic heating is often severe. As discussed in reference 1, the aerodynamic heating is often so severe that unprotected magnesium fins can be damaged enough to cause model instability that results in destruction of the model before completion of the flight test.

Since the basic magnesium fins were light, easy to fabricate, and efficient, it was decided to attempt to extend their usefulness under severe heating conditions. Consequently, an investigation was begun to determine the effectiveness of a number of protective-covering methods. Results of tests made to determine the relative effectiveness at high stagnation temperatures of several protective-covering methods applied to the fin leading-edge region are reported in reference 1. These tests were conducted by exposing uninstrumented models to a Mach number 2.0 airstream with an adjustable stagnation temperature.

Additional tests under similar conditions have been made with a series of eight instrumented models to determine the effectiveness of more elaborate protective coverings applied to the leading-edge region and protective coverings applied to the sides of the fins. Some effects of sweepback and leading-edge diameter on aerodynamic heating were also investigated.

The models were instrumented with thermocouples so that temperatures through successive layers of material and along the fin surfaces could be measured.

These tests were conducted at stream stagnation temperatures as high as $3,600^{\circ}$ R in the preflight high-temperature jet of the Langley Pilotless Aircraft Research Station at Wallops Island, Va.

SYMBOLS

c_w specific heat of material, $\text{Btu/lb} \cdot {}^{\circ}\text{R}$

G air gap, ft

K conductivity of air, $\frac{\text{Btu-ft}}{(\text{sec})(\text{sq ft})({}^{\circ}\text{R})}$

M	Mach number
q	total heat flux at a station, Btu/(sec)(sq ft)
T _w	temperature of material, °R
T _{so}	stagnation temperature of stream at jet center line, °R
t	time beginning when model reaches jet center line, sec
L.E.	leading edge
x/c	position of temperature measuring station behind leading edge, fraction of chord length
Λ	sweepback of fin leading edge, deg
ρ _w	density of material, lb/cu ft
τ _w	thickness of material, ft
Subscripts:	
1,2,3,4,5	temperature measuring stations
a,b,c	layers of material, a being outside layer, b middle layer, and c being inside layer

MODELS

The basic plan form chosen for this investigation was a trapezoidal fin that was fabricated from the same cast leading edges and the same magnesium plates currently being used to make booster fins. The leading edge was swept back 17° and the leading-edge half-wedge angle was 5.5°. As shown in figure 1, six models (models 1, 2, 3, 6, 7, and 8) were of the basic trapezoidal plan form, model 4 had a change in the sweep of the trailing edge, and model 5 was built with the leading edge swept back 45°. Models 1 and 6 had hexagonal airfoil sections with sharp trailing edges and the other models had slab airfoil sections behind the leading-edge wedge.

All the models were built with similar magnesium load-carrying structures to which protective layers of Inconel and stainless steel were added in various arrangements. Leading-edge and trailing-edge wedge sections were made of cast magnesium. Flat sections were fabricated

from 3/16-inch-thick magnesium plate. Details of the protective coverings applied to the models are as follows:

Models 1 and 6: A part of the leading-edge wedges of these models was wrapped with 1/32-inch-thick Inconel which was held in place with 1/8-inch-diameter rivets. In order to decrease the heat transfer between the Inconel and the magnesium, a piece of 0.008-inch-thick Fiberglas cloth was inserted between the metal surfaces of model 6.

Models 2 and 3: The leading-edge regions of these models were protected with 1/32-inch-thick Inconel in the same manner as model 1 except for changes in rivet spacing. The Inconel was held on model 3 by one rivet, near midspan, and a holder at the root which permitted spanwise movement and prevented chordwise movement of the Inconel cover.

Model 4: The leading-edge wedge of this model extended to the trailing edge and was completely covered with 1/32-inch-thick Inconel that was held in place by 1/8-inch-diameter steel rivets spaced about as shown in figure 1(d).

Model 5: A layer of 1/32-inch-thick Inconel was wrapped around the leading edge in the same manner as for models 1, 2, and 6.

Model 7: A 1/32-inch-thick piece of Inconel was wrapped around the leading edge and extended rearward to cover all the leading-edge wedge. The Inconel and magnesium surfaces were separated by a piece of 0.008-inch-thick Fiberglas cloth. Additional protection was obtained by wrapping a second layer of thicker Inconel (0.050 in.) around the leading edge. A layer of 0.003-inch-thick aluminum oxide was applied to the exposed magnesium on one side of this fin.

Model 8: All the side magnesium surfaces of this model were protected from high-temperature flow. A piece of 1/32-inch-thick Inconel was wrapped around the leading edge and extended rearward past the 50-percent chord line where it overlapped a piece of 1/64-inch-thick stainless steel that had been wrapped around the trailing edge. As for model 7, additional protection was obtained by wrapping a second layer of 0.050-inch-thick Inconel around the leading edge.

On all models the magnesium structure at the fin tip had no protective covering. The leading-edge radius was 1/16 inch for all the models tested, except for model 7, which had a leading-edge radius of 0.121 inch, and model 8, which had a leading-edge radius of 0.113 inch.

The weight penalty incurred by the protective coverings increased as the covering became more extensive. A 3.5-square-foot fin without protection weighed 14.0 pounds, or 4.0 pounds per square foot. With

protection like that used on models 1, 2, 3, 5, and 6 the fin weighed 4.3 pounds per square foot and with the protection used on model 7 the fin weight was increased to 5.2 pounds per square foot.

INSTRUMENTATION

Temperatures were measured at desired locations in the models with two different types of thermocouples: platinum-13-percent-platinum-rhodium and chromel-alumel thermocouples. Choice of thermocouples depended upon the maximum temperature expected at the station of application. Thermocouples were spot welded to the inside surfaces of the Inconel and stainless-steel pieces and were puddle welded into the magnesium surfaces.

The thermocouples were placed as close as practicable to the fin chord line that coincided with the center line of the jet when the model was in the testing position. This was done because the jet conditions varied across the stream with the most severe conditions occurring at the center line. Several models had thermocouples distributed spanwise at about 1/2-inch intervals along the leading edge.

Motion pictures of the model and of an electric clock were taken from one side and from overhead during each test at approximately 128 frames per second.

TESTS

The investigation was conducted by exposing the models at zero angle of attack in the 12-inch-diameter preflight high-temperature jet at a Mach number of 2.0. Each model was mounted on a stand that would insert it into the jet once the desired flow conditions had been established. Ten inches of the 11-inch span of each model were exposed in the jet, including the tip. The models were withdrawn from the jet at predetermined times or after damage to the fin was observed. The motion of the stand was such that a model traversed about one-half the diameter of the jet stream while being rotated to the test position and while being withdrawn. Approximately 0.4 second was spent traversing the jet stream in either direction.

The temperature varied across the diameter of the jet during these tests, the maximum temperature occurring near the center line, as discussed in reference 1. Calculated stream conditions based upon the center-line temperature immediately upstream of the model position are

presented in figure 2. A more detailed description of the operation and characteristics of the high-temperature jet is presented in reference 1.

The jet was operated so that the stream static pressure at the jet exit was 0.78 times the ambient pressure. This resulted in a total pressure of 9,780 pounds per square foot behind the detached shock waves which formed ahead of the 17° sweptback leading edges of the models. An equivalent pressure would be obtained in free flight at Mach numbers of 2.6 and 4.0 at altitudes of 20,000 feet and 40,000 feet, respectively.

Since the jet static pressure was less than ambient pressure, shock diamonds were formed near the exit and extended downstream to intersect on the jet center line about 2 inches (0.27 chord) behind the leading edge of the fins swept back 17° and 2 inches ahead of the leading edge of the fin swept back 45° .

During these tests most of the models remained in the jet until physical damage to the materials was observed. The physical condition of model 1 before the test and after 8 seconds in the jet at a stagnation temperature of about $3,500^\circ$ R is shown in figures 3(a) and 3(b), respectively.

Time histories of the temperatures measured on the models tested in this investigation are presented in figures 4 to 12. Stagnation temperatures for each test are included in the (a) part of each figure. Stagnation temperatures below $2,700^\circ$ R were measured on the jet center line; those above $2,700^\circ$ R were obtained by extrapolating temperatures measured in the cooler regions of the jet off the center line (ref. 1). Whenever available, the temperatures of the basic magnesium structure and intermediate layers of protective coverings at the same station are included with temperatures of the outside protective covering. The time histories are presented to the time of thermocouple or model failure.

RESULTS AND CALCULATIONS

Simple Leading-Edge Protection (Models 1 to 5)

As indicated by the qualitative results of reference 1, wrapping the leading-edge region with $1/32$ -inch-thick Inconel was a very effective scheme for protecting the magnesium structure from the effects of severe aerodynamic heating. A similar protective arrangement was used during the present investigation on models 1, 2, 3, and 5. The thermocouple measurements presented in figures 4(a), 5(a), and 6(a) show a large difference between the temperature of the Inconel covering at the leading edge and the temperature of the adjacent magnesium structure. A smaller,

but still significant, temperature difference was measured on the wedge section behind the leading edge (station $x/c = 0.133$) of model 1 (fig. 4(b)).

Destruction of model 1, which was tested under more severe conditions than models 2 and 3, is attributed to failure of the Inconel cover at the fin leading edge at about 2.0 seconds. Measured temperatures at the leading edge, while not constant along the span because of the stagnation temperature gradient across the jet, indicate temperatures higher than the melting temperature of Inconel ($2,960^{\circ}$ R) at two stations. These extraordinarily high temperatures could possibly have been caused by oxidation of the Inconel at local spots on the leading edge. Just before the leading-edge cover failed, it was observed that the sharp trailing edge started to melt at several locations near the jet center line.

At the end of the test the temperature of the magnesium at the leading edge of models 1 to 3 had increased to more than $1,300^{\circ}$ R. (Magnesium melts at about $1,660^{\circ}$ R.) Temperature of the exposed magnesium farther to the rear of these models approached the melting temperature, particularly on models 2 and 3, which lasted longer than model 1. The first damage observed on these two models was surface melting of the exposed magnesium at about 2.0 seconds. Burning was observed on model 2 at about 4.6 seconds and on model 3 at about 3.5 seconds at the places where surface melting was observed. (According to ref. 2, under the conditions of these tests, magnesium can ignite at temperatures near the melting temperature.) Some free oxygen, as listed in table I, was present during each test and varied with stagnation temperature as shown in reference 1.

The protective covering at the leading edge of model 4 was identical to that on models 1, 2, and 3 but extended all the way to the trailing edge. Similar to model 1, model 4 was subjected to more severe test conditions than models 2 and 3. The stagnation temperature of this test was about the same as that for model 1 and the temperature measured on the Inconel leading edge (fig. 7(a)) increased at about the same rate as the higher temperature measurements at the leading edge of model 1. The temperature at this one measuring station had not reached the melting point of Inconel when the Inconel cover was observed to fail along the leading edge as in the case of model 1. This indicated that the temperature at stations away from the measuring station were probably higher than the melting temperature.

Temperatures were also measured along the wedge of model 4, as shown in figure 7(b). On the near side of the fin the magnesium structure in

a plug approximately 1.5 inches in diameter was removed to the airfoil chord plane. A thermocouple was attached at the center of the Inconel covering the cavity. Thermocouples were also placed in the Inconel and adjacent magnesium at the corresponding location on the far side of the fin. Comparison of the near-side temperature measurements with the somewhat limited far-side measurements indicates the large amount of heat that can be conducted from a hot piece of Inconel to the adjacent magnesium in a simple structure.

A simple leading-edge protective covering was also used on model 5, which had the leading edge swept back 45° . Streamwise structural details remained the same as those on the previous models (except model 4), since the increase in sweep of the leading edge was obtained by shearing the wing sections in planes aligned with the free-stream direction.

Temperatures measured at the leading edge during the test, which was conducted at a stagnation temperature of about $3,400^\circ R$, increased only a little less rapidly than the temperatures measured during the tests of models 1 to 4, thus roughly indicating that the same amount of heat was transferred from the stream to the leading edges of models with 17° and 45° of sweepback. However, it should be noted that the leading edge of model 5 was in the flow region downstream of the tunnel-exit-shock intersection point instead of upstream as were the leading edges of models 1 to 4. Thus, the decrease in heat transfer that would be expected from an increase in sweepback angle was probably offset by the more severe stream conditions imposed on the leading edge of model 5. Temperatures measured in the exposed magnesium at the midchord position were about the same as temperatures at the same position and comparable times on other models in this group.

First damage to the fin was observed at about 1.9 seconds when surface melting on the magnesium behind the Inconel cover occurred. Near the time of model destruction the unprotected magnesium at the tip (near the leading edge) was observed to ignite. Shortly thereafter, at about 3.2 seconds, the magnesium (where surface melting was first observed) began to burn and the fin failed.

From the tests of models 1 to 5 it can be seen that the simple leading-edge protection did protect the adjacent magnesium surfaces. It was also seen that the protection was just sufficient for the test conditions; that is, for the more severe tests, models 1 and 4, the Inconel failed from overheating before the protected magnesium had attained melting temperature. For less severe tests, models 2, 3, and 5, the model lasted a little longer but still failed when the unprotected magnesium behind the leading edge ignited.

Modified Simple Leading-Edge Protection (Model 6)

In order to investigate the effects of using an insulator to decrease the transfer of heat from the hot protective coverings to the adjacent magnesium structure, a model identical to model 1 was built with one layer of 0.008-inch-thick Fiberglas cloth separating the Inconel from the magnesium. Temperature time histories obtained during the test of this model at only slightly lower stagnation temperatures than those attained during the test of model 1 are presented in figure 9. At the leading edge and at station $x/c = 0.133$ (along the wedge) the temperature rise in the magnesium was only about 35 percent and 27 percent, respectively, that of model 1 after about 1.5 seconds (time of failure of model 6). Other evidence that more heat was retained in the Inconel was obtained from high-speed motion pictures of the test, which showed that the Inconel cover on model 6 heated sooner and failed sooner than the cover on model 1. This meant that the temperature of the cover on model 6 reached melting temperature first, even though the only temperature measured on the cover of model 6 was well below the melting temperature; the measured temperature at the corresponding location on model 1 was also less than the melting temperature of Inconel at the time of model failure. This difference probably resulted from local flow nonuniformities in the jet. Thus, for the conditions imposed, it can be seen that reducing the transfer of heat to the magnesium structure shortened the useful life of the Inconel cover.

Temperatures of the exposed magnesium at midchord on model 6 were about the same as those on model 1 at comparable times, but the temperature at the trailing edge increased faster and had exceeded $1,500^{\circ}$ R at the end of the test. From the films of the test it was observed that the magnesium near the thermocouple installation on the sharp trailing edge started to melt at about the time the Inconel leading-edge cover failed.

Double-Wrapped Leading Edge (Model 7)

In an effort to obtain protection for the magnesium structure that would have greater duration, model 7 was designed. This model was somewhat similar to model 6 except the 1/32-inch-thick Inconel cover and the layer of Fiberglas were extended rearward to completely cover the leading-edge wedge where models 2, 3, and 5 experienced initial difficulties. In order to provide additional protection at the leading edge, where models 1, 4, and 6 had experienced initial failures, an additional cover of 0.050-inch-thick Inconel was wrapped around the leading edge.

This model was tested twice at stagnation temperatures near $2,500^{\circ}$ R, considerably lower than the stagnation temperatures of the tests previously discussed, once for 4 seconds and again for 10 seconds. Measured

temperatures as shown in figures 10 and 11 were of about the same magnitude in both tests. The temperature of the magnesium under the Inconel covers remained low all during the tests. Even at the end of the 10-second test the temperature of the magnesium at the leading edge had only increased 400° R.

Temperatures measured in the magnesium rearward of the Inconel covers (fig. 11(c)) show that the magnesium, particularly at the most rearward station, was approaching its melting temperature at the end of the 10-second test; and inspection of the model after this test showed that local magnesium surface melting had occurred at this station. On the other side of the fin, where a layer of aluminum oxide about 0.003 inch thick covered the magnesium surface, temperatures measured in the magnesium at comparable stations and local surface melting were about the same.

Fully Clad Fin (Model 8)

Results of the tests of the other models showed that model failure was precipitated either by failure of the simple Inconel covers at the leading edge or by melting, and possibly burning, of the exposed magnesium surfaces along the sides of the fins. These apparent weak spots were reinforced on model 8 by placing protective coverings over the entire side areas of the fin, 1/32-inch-thick Inconel on the forward section and 1/64-inch-thick stainless steel on the rear section. Additional protection at the leading edge was obtained by adding a short-chord cover of 0.050-inch-thick Inconel around the leading edge.

The model was tested to destruction with the jet at a stagnation temperature of about 3,400° R. This model lasted for more than 8 seconds which was much longer than other models lasted at this stagnation-temperature level and almost as long as model 7 which suffered some damage after 10 seconds at a stagnation temperature of only 2,400° R. Most of the protective covering on model 8 became red hot after 3 seconds in the jet, but the temperature of the magnesium under the covering remained relatively low (fig. 12). The temperature measurements obtained during the test of this model are presented in figure 12 to illustrate the effectiveness of the protective coverings applied at the different locations.

It was observed that the destruction of the model was precipitated by failure of the outer Inconel cover at the leading edge near the jet center line.

Relative Effectiveness of Protective Covers

Results of tests of three models (1, 6, and 8) which were tested at nearly the same stagnation temperatures, are presented in figure 13 to illustrate the relative effectiveness of three types of protective coverings used. Comparing the temperatures measured on the magnesium under the coverings at the leading edge and at station $x/c = 0.133$ along the wedge shows that the double-wrapped protection of model 8 gave more protection, particularly at the leading edge, than the modified simple leading-edge protection of model 6 and the simple leading-edge protection of model 1. Also, by comparing results of models 1 and 6, it can be seen how effective the layer of Fiberglas inserted between the Inconel cover and the magnesium on model 6 was in decreasing the temperatures of the protected magnesium. The protection given by the double-wrapped leading edge of model 8 was so much better than that given by the simple leading-edge protection of model 1 that at the leading edge the temperature rise measured in the magnesium of model 1 was reduced 97 percent in model 8 at the time of failure of model 1.

Heat Flux

Some idea of the severity of these tests can be obtained from the time histories of the total heat flux to various stations on models 3 and 8 presented in figure 14. Maximum values shown are about the same as those calculated for the most severe heating conditions encountered by fin-stabilized flight models. The values of heat flux represent the sum of the changes in heat content in each layer of fin material at a particular station. The changes in heat content of each layer were obtained by assuming that the measured temperature of each layer represented the average through the layer. Thus, the heat-flux values calculated for the models with the thickest protective coverings (like model 8) can be expected to be somewhat low, since they are the ones most influenced by the temperature difference obtained through Inconel because of its poor heat-conducting properties.

The difference in magnitudes of the leading-edge heat flux for models 3 and 8 can also be partly attributed to the larger leading-edge diameter of model 8 which decreased the magnitude of the aerodynamic heat-transfer coefficient.

Test stagnation temperatures, protective coverings, and results of the tests of the eight models are summarized in table I.

Calculations

Experimentally determined values of total heat flux were used to calculate the size of the effective gaps between each layer. Assumptions made to perform the calculations are as follows: (1) heat was transferred across air gaps by conduction only, (2) the temperature of the air in a gap was taken as the average temperature of the surfaces bounding a gap, and (3) no temperature gradient existed through the Inconel or in the magnesium. Equations used to calculate the size of the gaps were

$$q - \frac{K_{a-b}}{G_{a-b}}(T_{w,a} - T_{w,b}) = \rho_{w,a} \tau_{w,a} c_{w,a} \frac{\Delta T_{w,a}}{\Delta t}$$

$$\frac{K_{a-b}}{G_{a-b}}(T_{w,a} - T_{w,b}) - \frac{K_{b-c}}{G_{b-c}}(T_{w,b} - T_{w,c}) = \rho_{w,b} \tau_{w,b} c_{w,b} \frac{\Delta T_{w,b}}{\Delta t}$$

$$\frac{K_{b-c}}{G_{b-c}}(T_{w,b} - T_{w,c}) = \rho_{w,c} \tau_{w,c} c_{w,c} \frac{\Delta T_{w,c}}{\Delta t}$$

All three equations were used when calculating temperatures in a model with two protective layers like those on models 7 and 8. When only one protective layer was considered, the symbols with subscript *c* were omitted.

Sizes of the effective gaps were established by solving these equations with assumed values for gap size until values were found that resulted in temperature-time histories in the layers that agreed well with experimental results. Sizes of calculated effective gaps are presented in the following table:

Model	G_{a-b} , in.	G_{b-c} , in.	Location
2	.0400	-----	Leading edge
3	.0400	-----	Leading edge
5	.0100	-----	Leading edge
7	.0035	0.0100	Leading edge
8	.0035	.0100	Leading edge
8	.0035	.0015	x/c = 0.133

It may be noted that these values are all greater than the minimum average air gap to be expected between two metallic surfaces, 0.0005 inch, as given in reference 3. As indicated by the numbers in the table, the largest gaps can be expected when the radius of curvature is smallest.

Calculated temperatures of the two layers of protective covering and of the magnesium at the leading edge of model 8 as made with the gap sizes listed in the preceding table are compared in figure 15 with the measured temperatures. It should be noted that the agreement between the temperature curves was good to the time the calculations were terminated.

The effect of gap magnitude on the temperatures calculated for model 3 can be seen in figure 16. Calculated temperatures for gaps of 0.02 inch and 0.08 inch are compared with the temperatures calculated for a gap of 0.04 inch, which showed good agreement with experiment. Increasing the gap raised the temperature of the Inconel cover and decreased the temperature of the magnesium. Decreasing the gap had an opposite effect. A comparison of these calculated temperatures shows that a factor of 2 difference in gap magnitude caused temperature changes as much as 270° R in the magnesium and 40° R in the Inconel at a time of 2.25 seconds.

CONCLUSIONS

Eight magnesium fins with various protective coverings designed to alleviate aerodynamic-heating effects have been tested in a high-temperature jet at a Mach number of 2.0. Results of nine tests at stagnation temperatures up to $3,600^{\circ}$ R indicate the following conclusions:

1. Wrapping Inconel around the fin leading edges protected the adjacent magnesium structure to the melting temperature of the Inconel covering. For less severe tests the fin lasted longer but the exposed magnesium surfaces behind the Inconel covering ignited.
2. Increasing the protective covering at the leading edge and extending protection over the exposed magnesium surfaces made the basic magnesium fin as much as four times as durable at stagnation temperatures as high as $3,400^{\circ}$ R.

3. Inserting a piece of Fiberglas between the Inconel cover and the magnesium appeared to decrease materially the amount of heat transferred from the Inconel to the magnesium.

Langley Aeronautical Laboratory,
National Advisory Committee for Aeronautics,
Langley Field, Va., September 30, 1957.

REFERENCES

1. Bland, William M., Jr., and Bressette, Walter E.: Some Effects of Heat Transfer at Mach Number 2.0 at Stagnation Temperatures Between $2,310^{\circ}$ and $3,500^{\circ}$ R on a Magnesium Fin With Several Leading-Edge Modifications. NACA RM L57C14, 1957.
2. Hill, Paul R., Adamson, David, Foland, Douglas H., and Bressette, Walter E.: High-Temperature Oxidation and Ignition of Metals. NACA RM L55L23b, 1956.
3. Eckert, E. R. G. (with Appendix by Robert M. Drake, Jr.): Introduction to the Transfer of Heat and Mass. First ed., McGraw-Hill Book Co., Inc., 1950.

TABLE I

SUMMARY OF TEST CONDITIONS AND RESULTS

Model	Λ , deg	Protection	Stagnation temperature range, $^{\circ}\text{R}$	Calculated amount of free oxygen in stream by volume, percent	Time of failure, sec	Maximum measured temperature in Inconel cover, $^{\circ}\text{R}$	Remarks
1	17	Simple L.E. - 1/32-inch-thick Inconel cover (fig. 1(a))	3,460 to 3,480	7.5	2.0	3,120	Inconel cover failed at 2.0 seconds. Magnesium was observed to melt at sharp T.E. before this time.
2	17	Simple L.E. - 1/32-inch-thick Inconel cover (fig. 1(b))	2,980 to 3,360	9.4	4.6	2,630	Exposed magnesium behind L.E. cover melted at 2.0 seconds and ignited at 4.6 seconds.
3	17	Simple L.E. - 1/32-inch-thick Inconel cover (fig. 1(c))	3,210 to 3,320	8.6	3.5	2,960	Exposed magnesium behind L.E. cover melted at 2.0 seconds and ignited at 3.5 seconds.
4	17	Simple L.E. - 1/32-inch-thick Inconel cover to trailing edge (fig. 1(d))	3,550 to 3,600	6.9	1.6	2,850	Inconel cover failed along stagnation line.
5	45	Simple L.E. - 1/32-inch-thick Inconel cover (fig. 1(e))	3,350 to 3,400	7.9	3.2	2,800	Exposed magnesium behind L.E. cover melted at about 1.9 seconds and ignited at 3.2 seconds. Exposed magnesium at tip ignited at about 3.0 seconds.
6	17	Modified simple L.E. - 1/32-inch- thick Inconel cover and Fiberglas (fig. 1(a))	3,380 to 3,430	7.8	1.5	2,100	Inconel cover failed along stagnation line.
7	17	Double-wrapped L.E. (fig. 1(f))	2,380 to 2,440	13.0	--- (4 second test)	1,740	No damage.
7	17	Double-wrapped L.E. (fig. 1(f))	2,410 to 2,560	12.6	--- (10 second test)	2,000	Some melting of exposed magnesium noted at end of test.
8	17	Fully clad fin with double-wrapped L.E. (fig. 1(g))	3,310 to 3,490	7.8	8+	2,300	Most of covering was red hot at 3 seconds. L.E. cover failed along stagnation line at about 8.4 seconds.

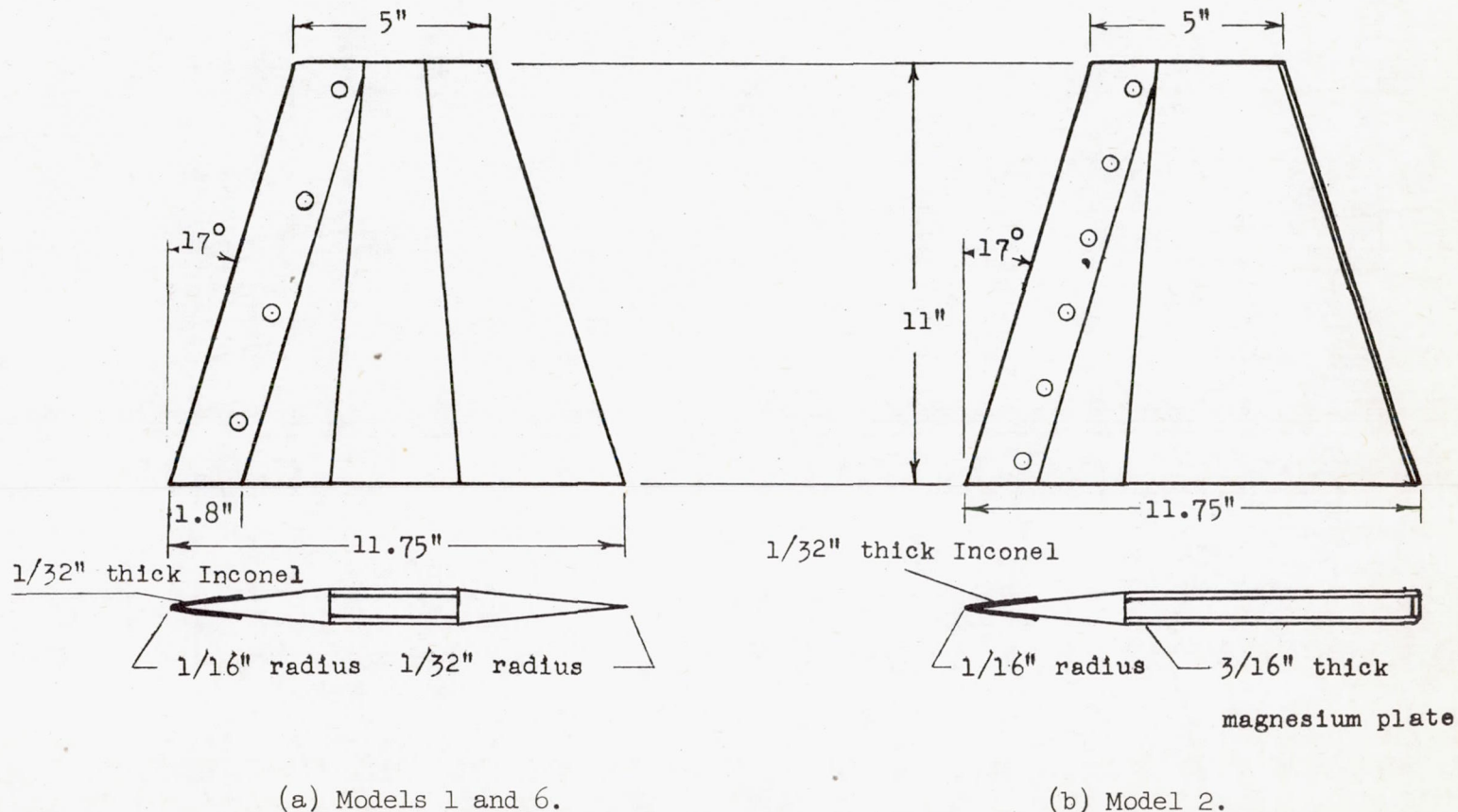
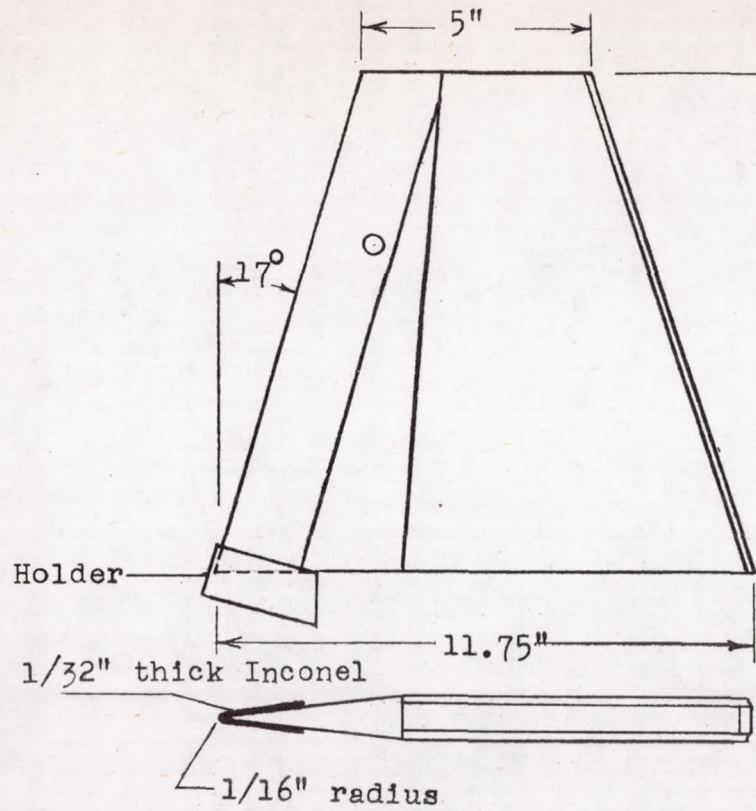
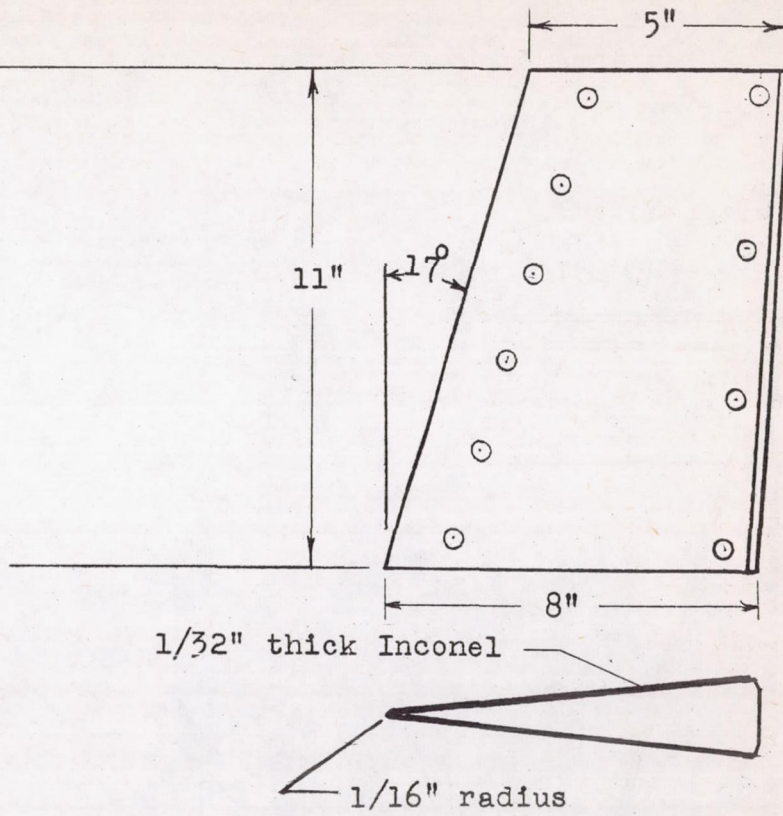


Figure 1.- Sketches of models tested. Rivet patterns are shown to scale.

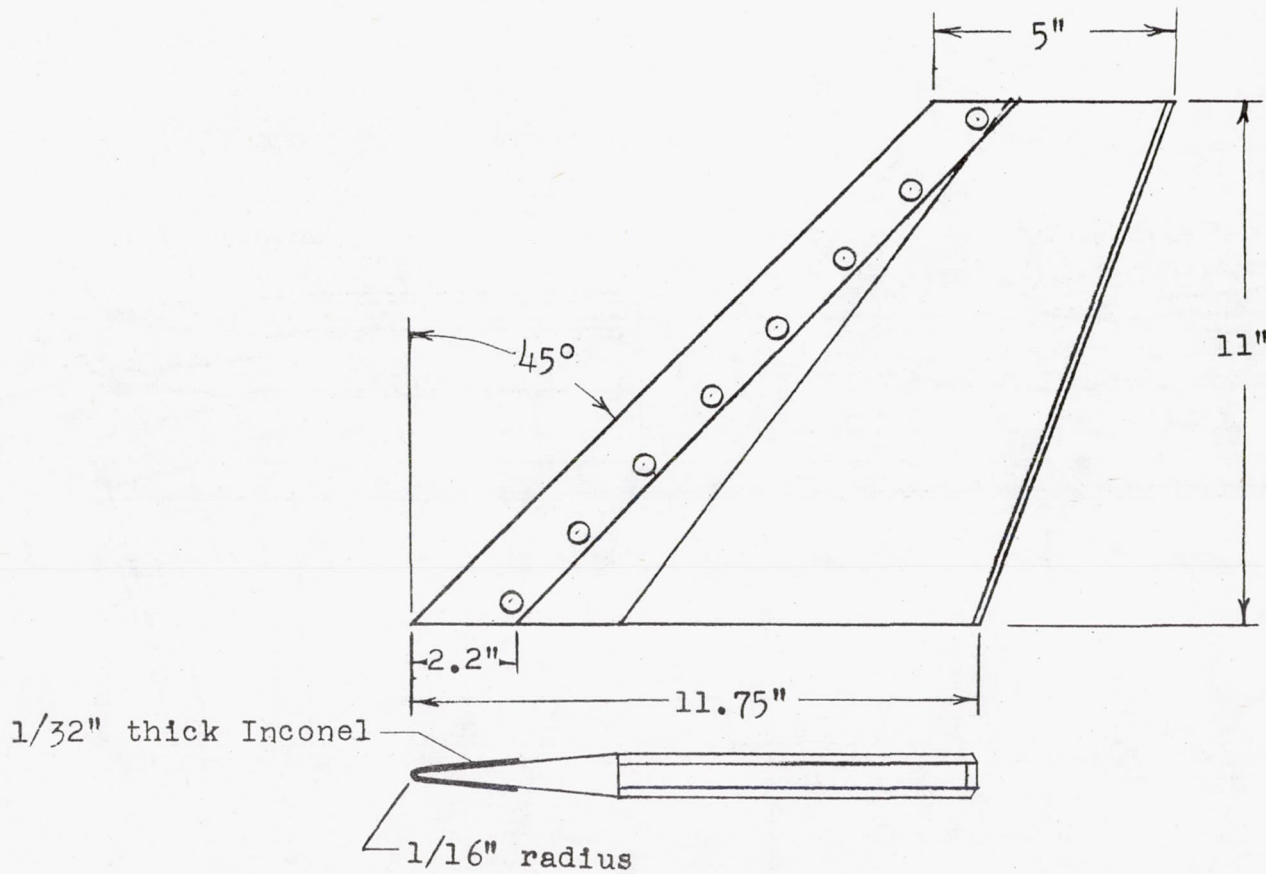


(c) Model 3.



(d) Model 4.

Figure 1.- Continued.



(e) Model 5.

Figure 1.- Continued.

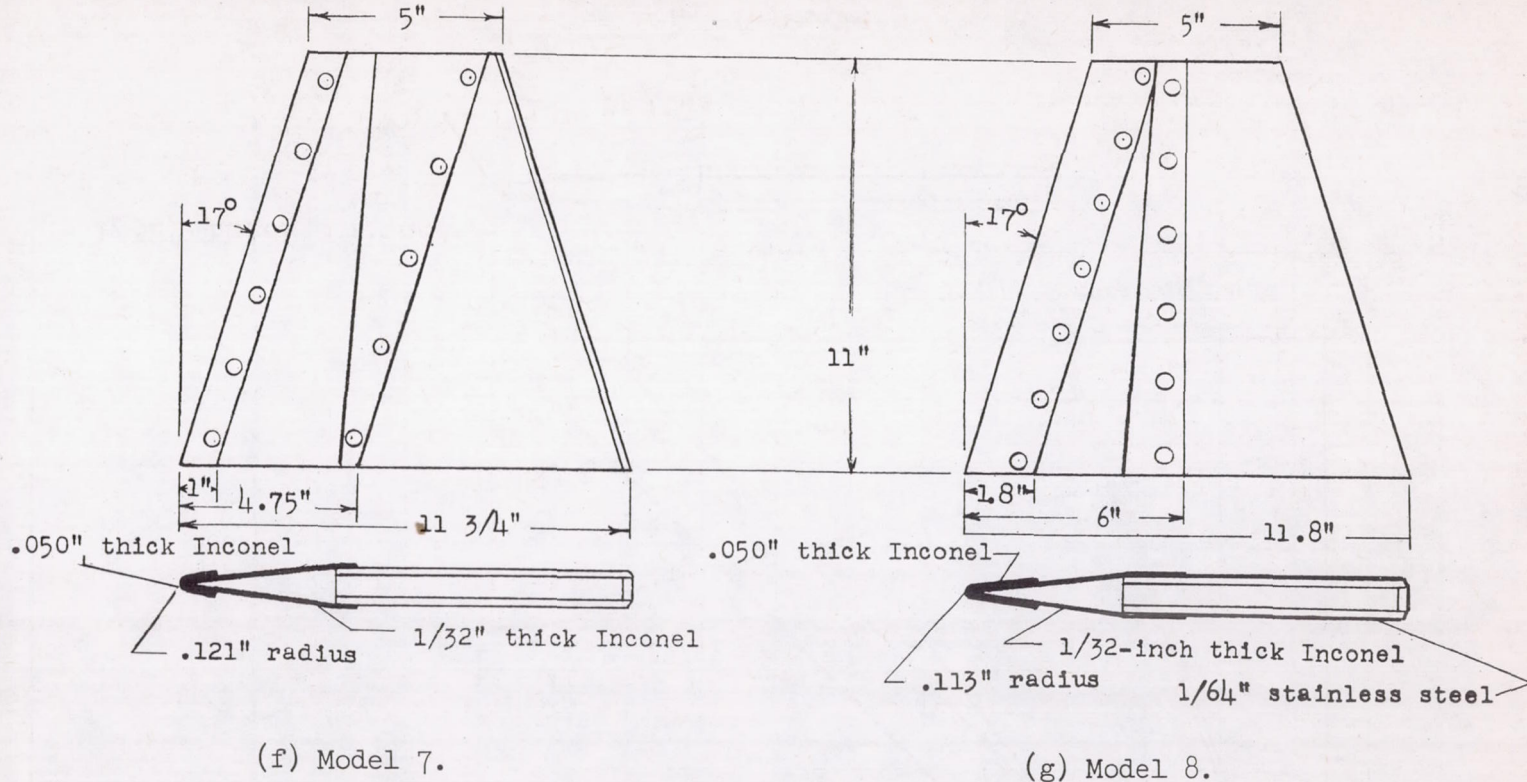
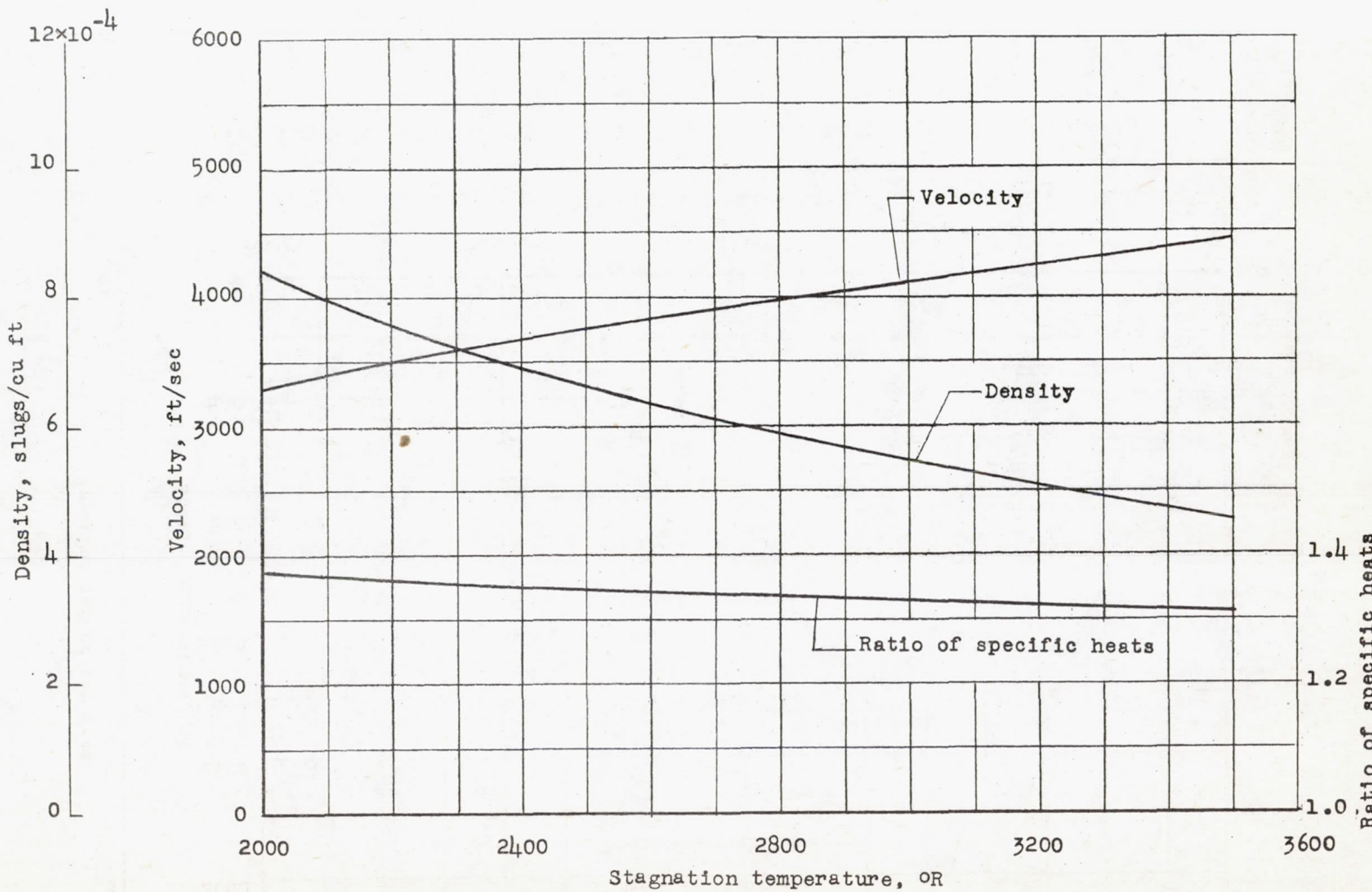
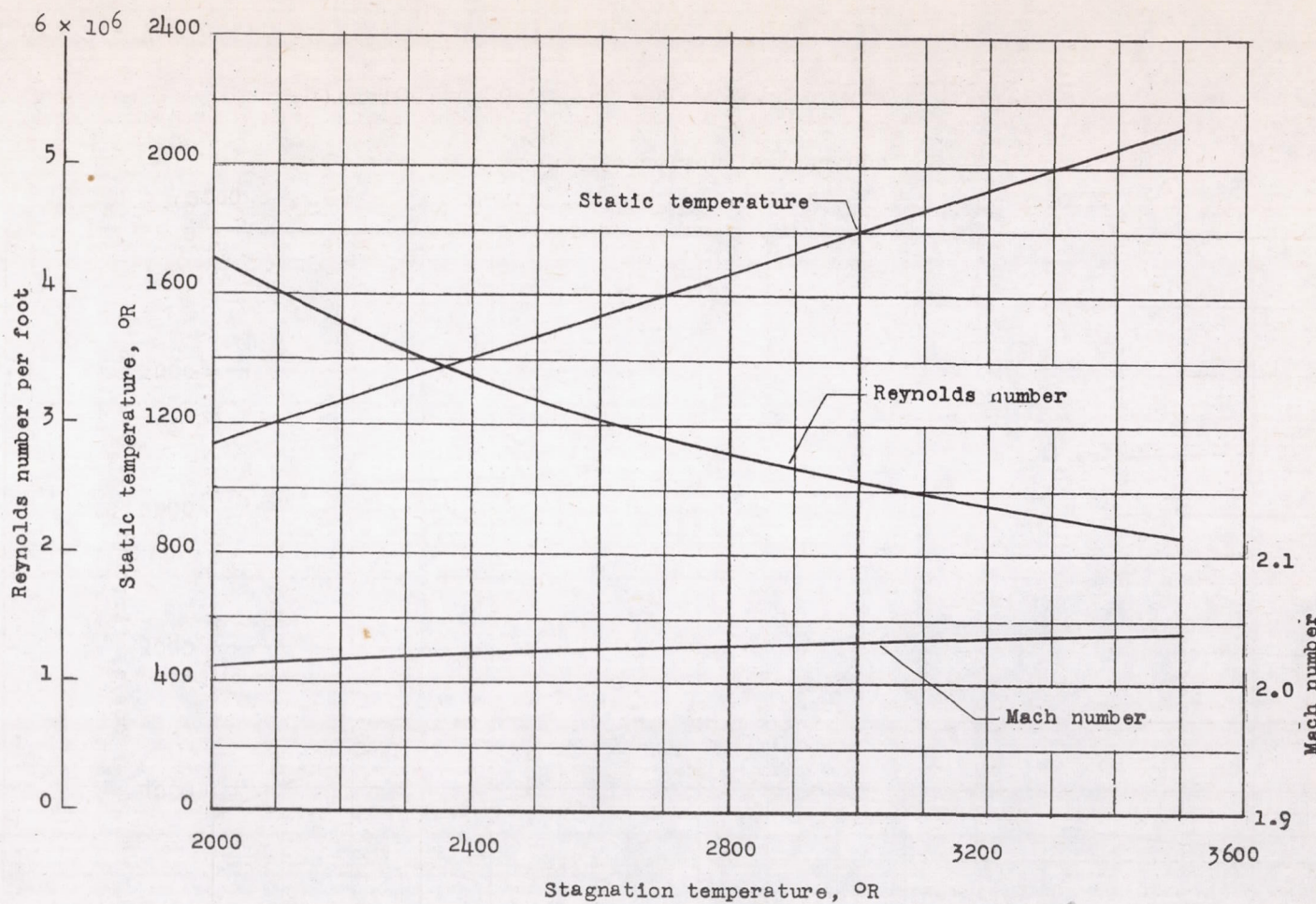


Figure 1.- Concluded.



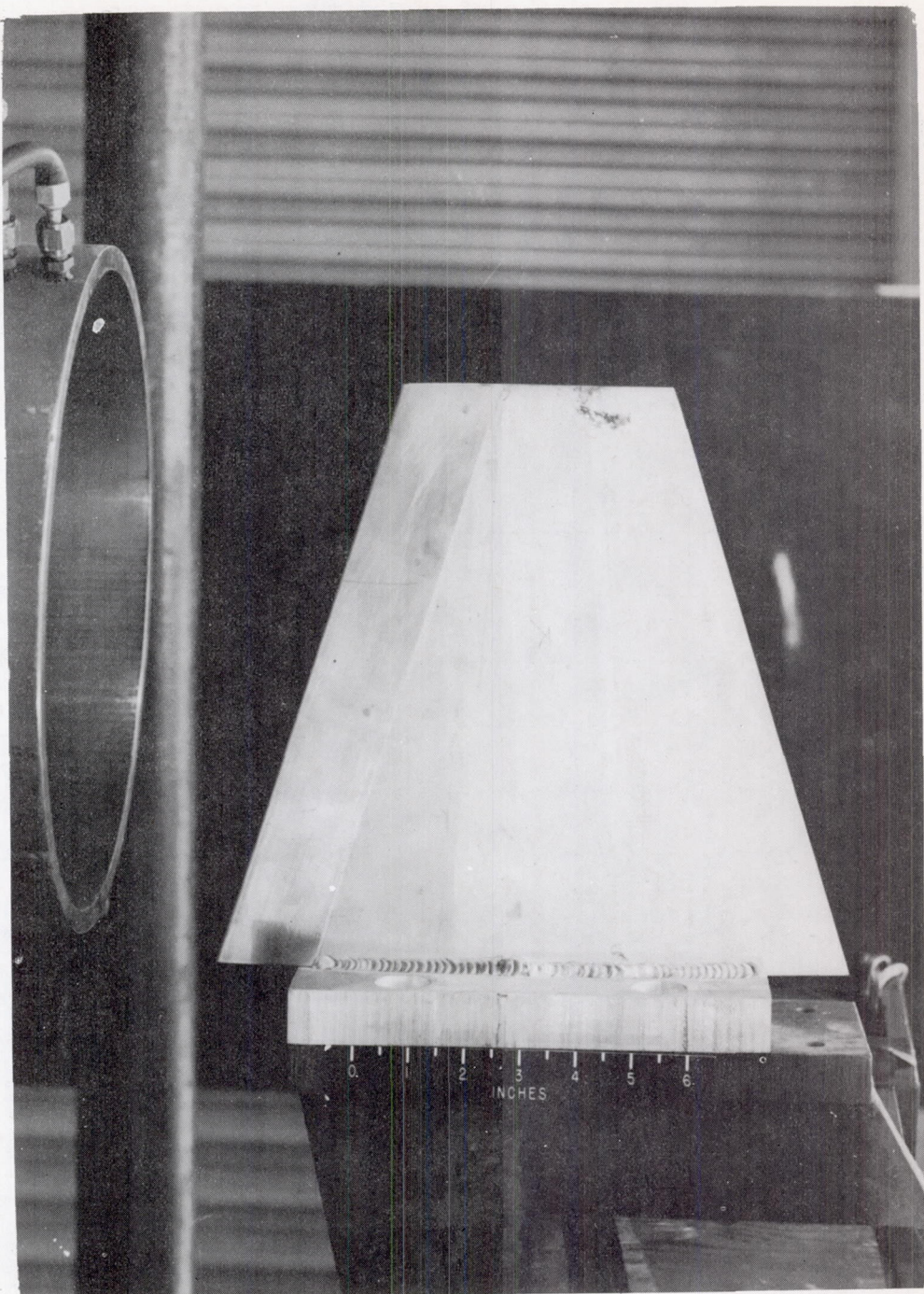
(a) Velocity, density, and ratio of specific heats.

Figure 2.- Variation of stream conditions along jet center line with stagnation temperature.



(b) Reynolds number per foot, static temperature, and Mach number.

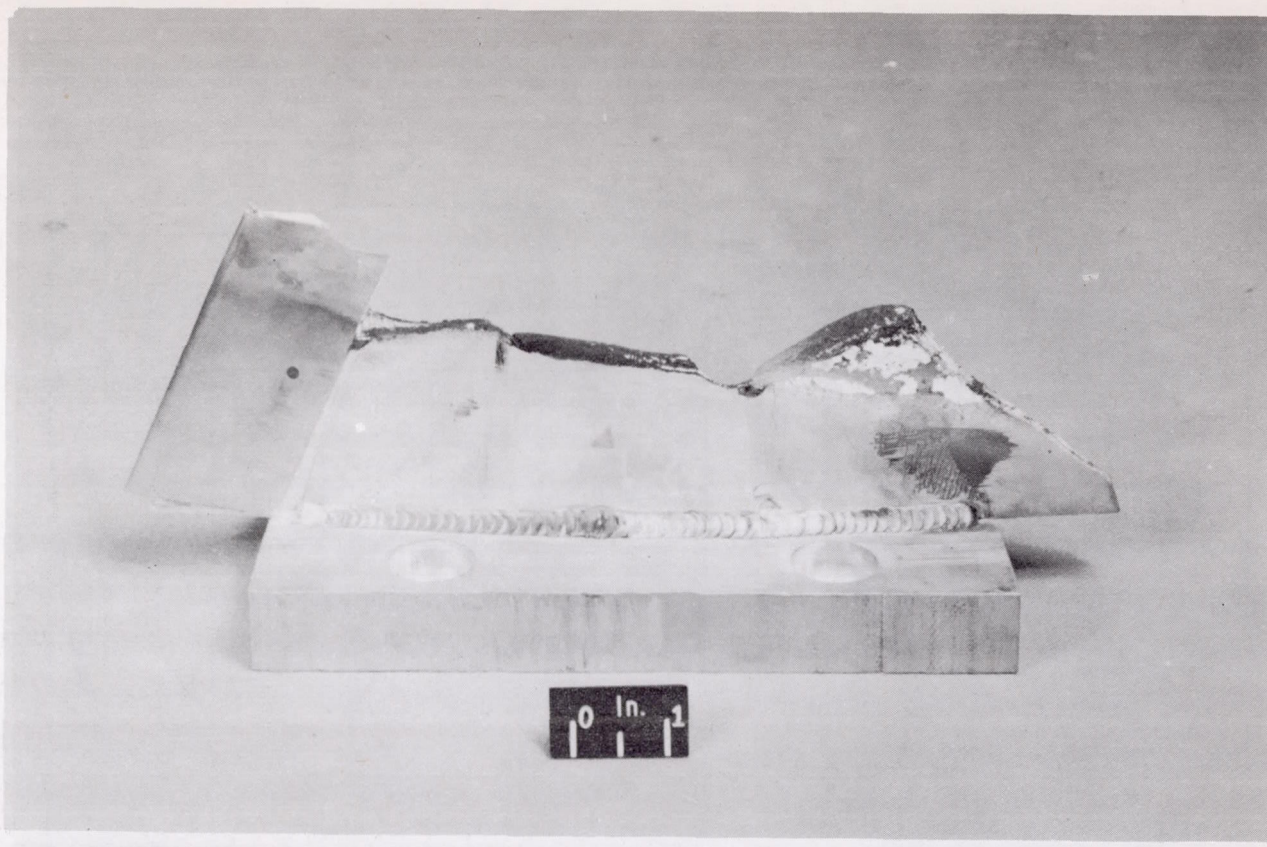
Figure 2.- Concluded.



(a) In testing position before test.

L-94737.1

Figure 3.- Model 1.



L-94945.1

(b) After exposure in jet for 8 seconds at stagnation temperature of
about $3,500^{\circ}$ R.

Figure 3.- Concluded.

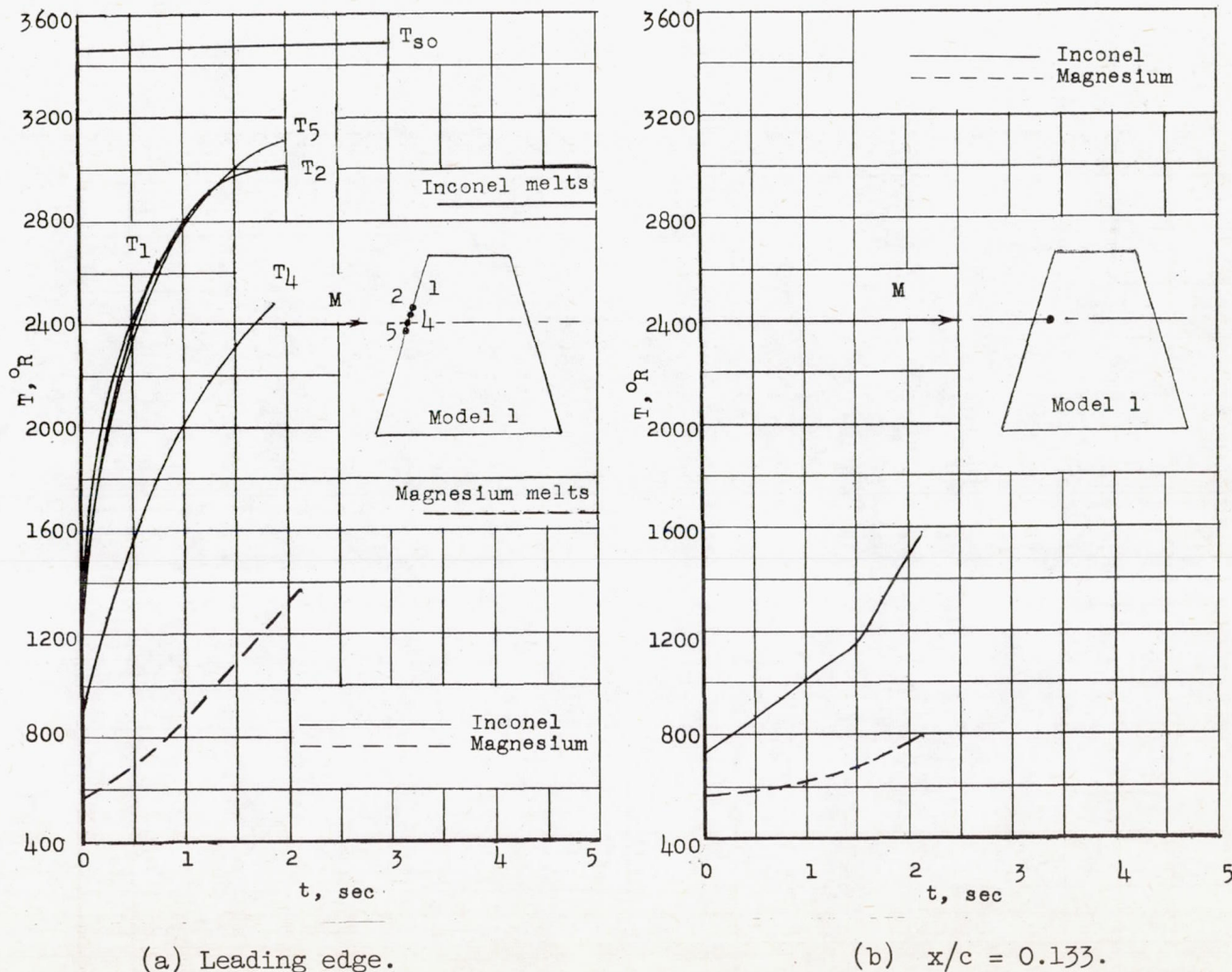


Figure 4.- Temperature time histories obtained during test of model 1. Free oxygen in stream about 7.5 percent by volume.

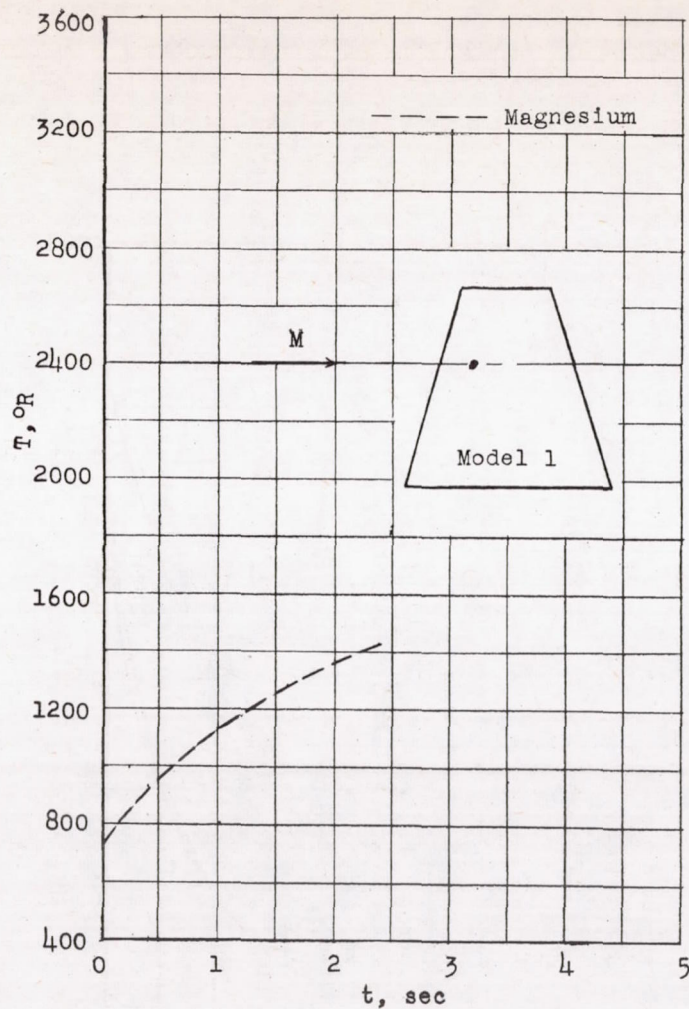
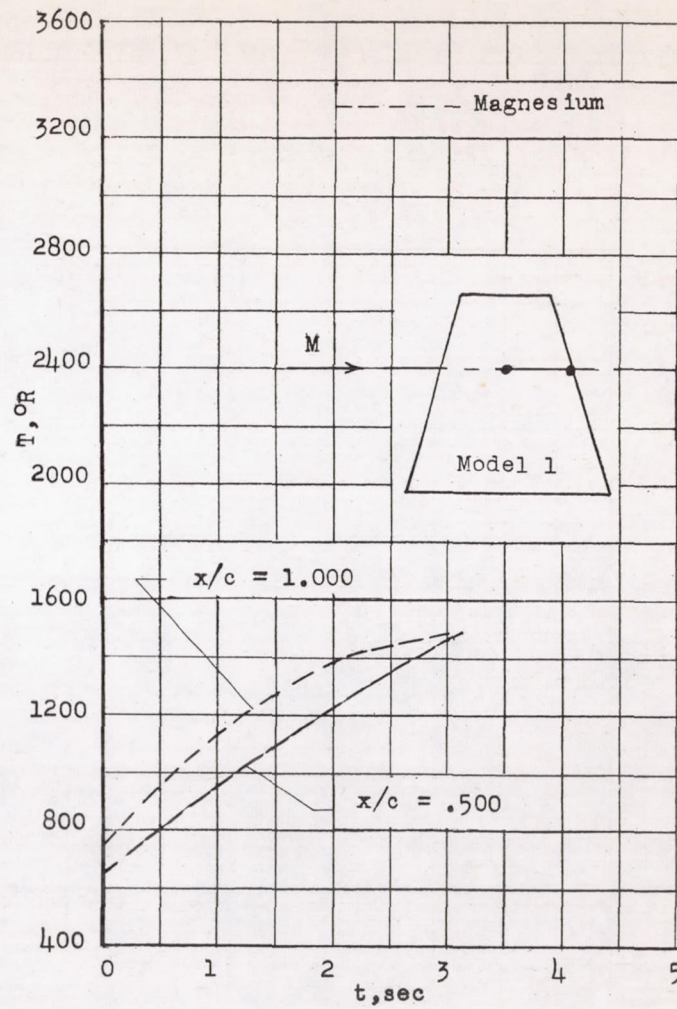
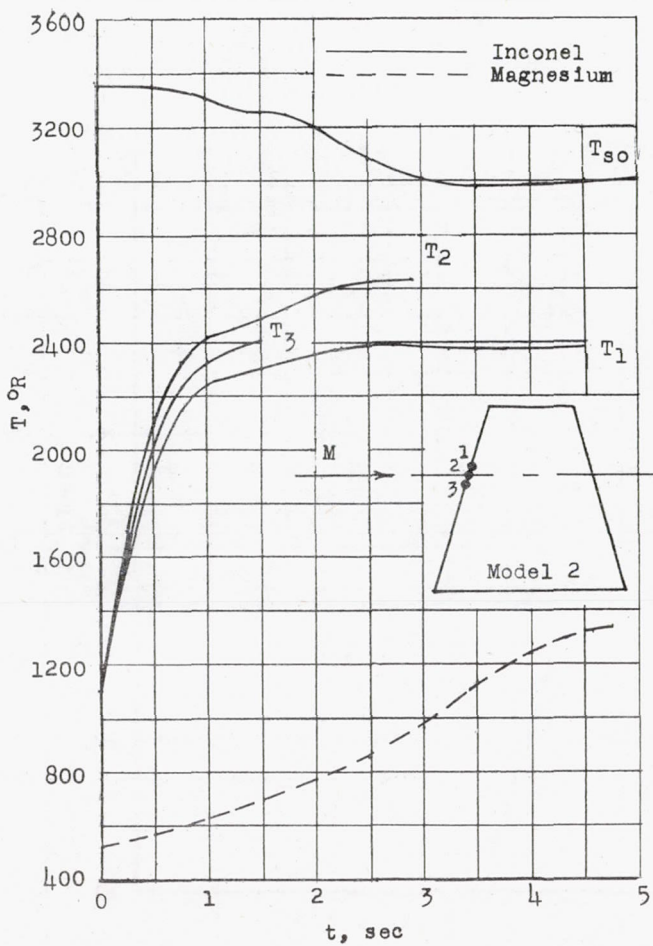
(c) $x/c = 0.266.$ (d) $x/c = 0.500$ and $x/c = 1.00.$

Figure 4.- Concluded.



(a) Leading edge.

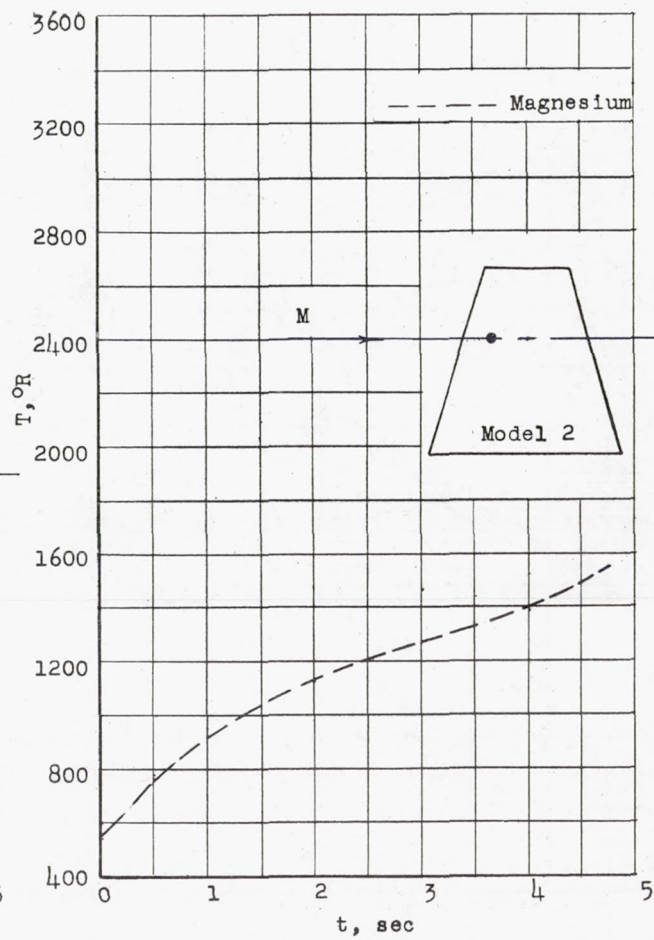
(b) $x/c = 0.266$.

Figure 5.- Temperature time histories obtained during test of model 2. Free oxygen in stream about 9.4 percent by volume.

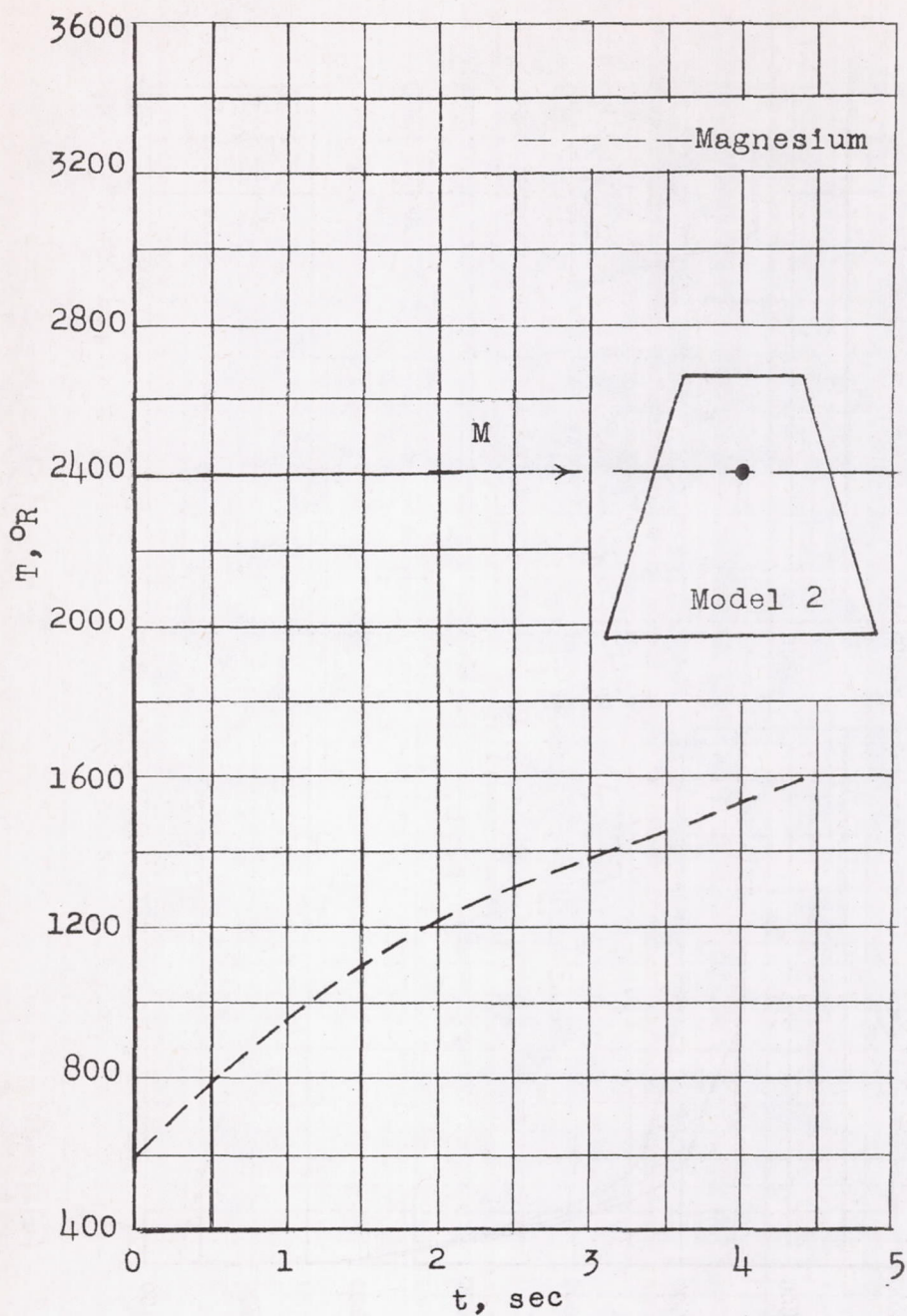
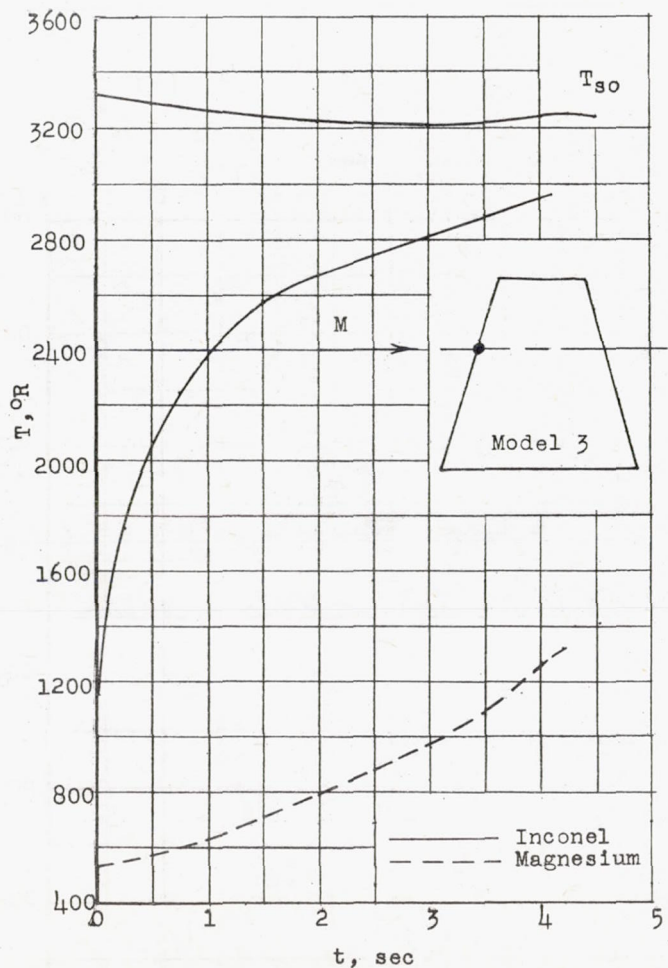
(c) $x/c = 0.500$.

Figure 5.- Concluded.



(a) Leading edge.

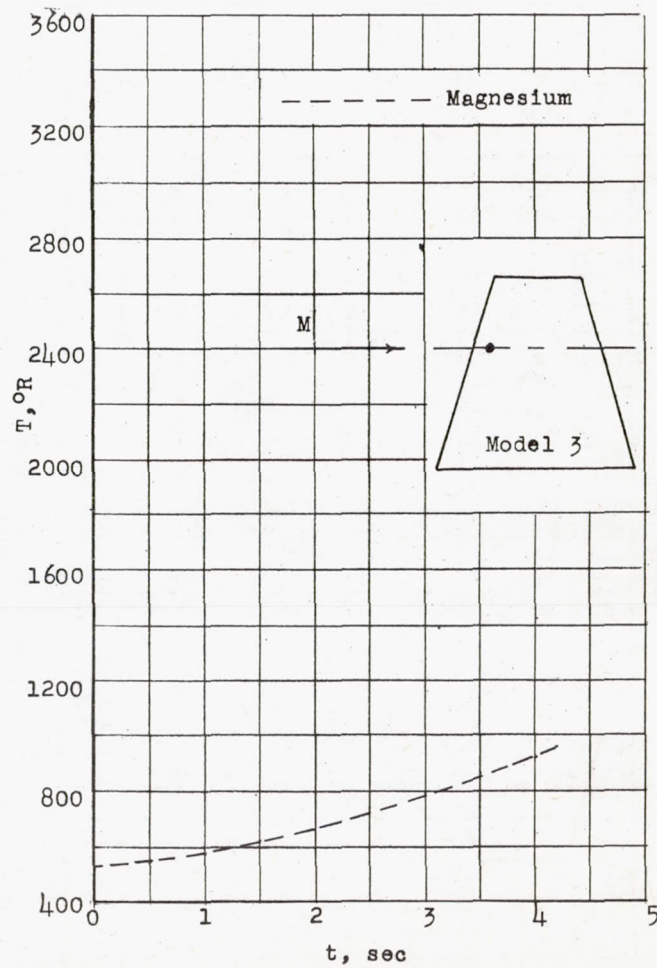
(b) $x/c = 0.133$.

Figure 6.- Temperature time histories obtained during test of model 3. Free oxygen in stream about 8.6 percent by volume.

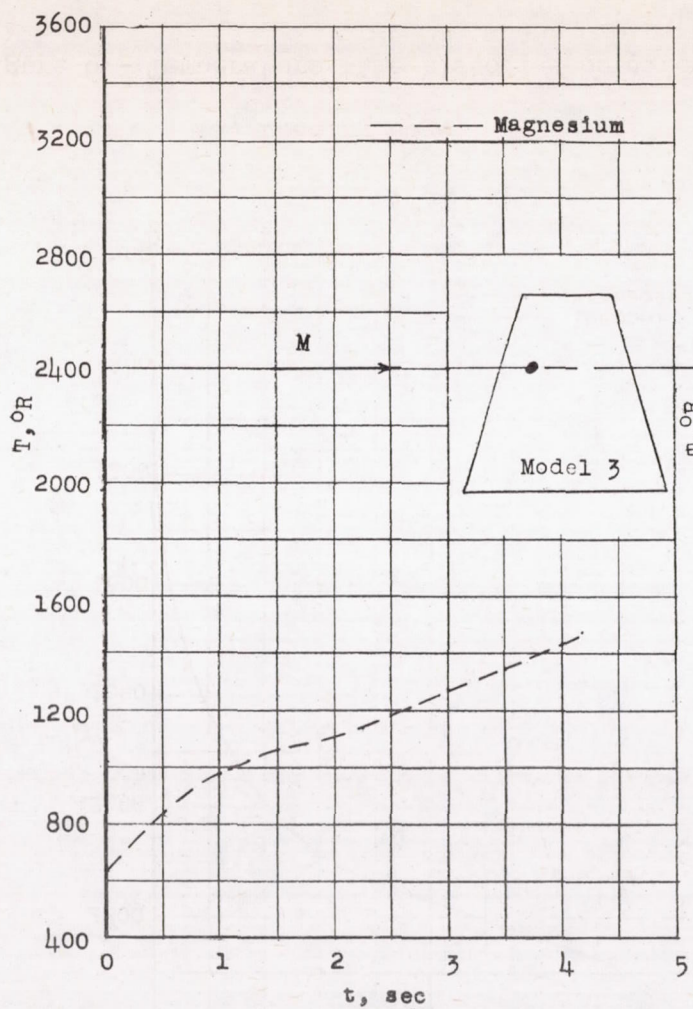
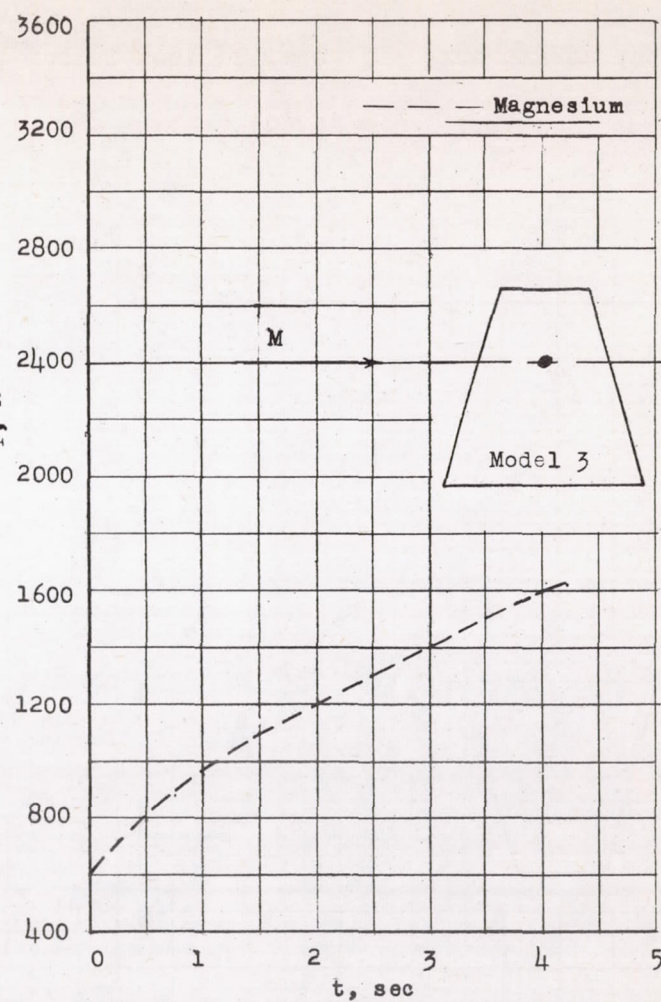
(c) $x/c = 0.233$.(d) $x/c = 0.500$.

Figure 6.- Concluded.

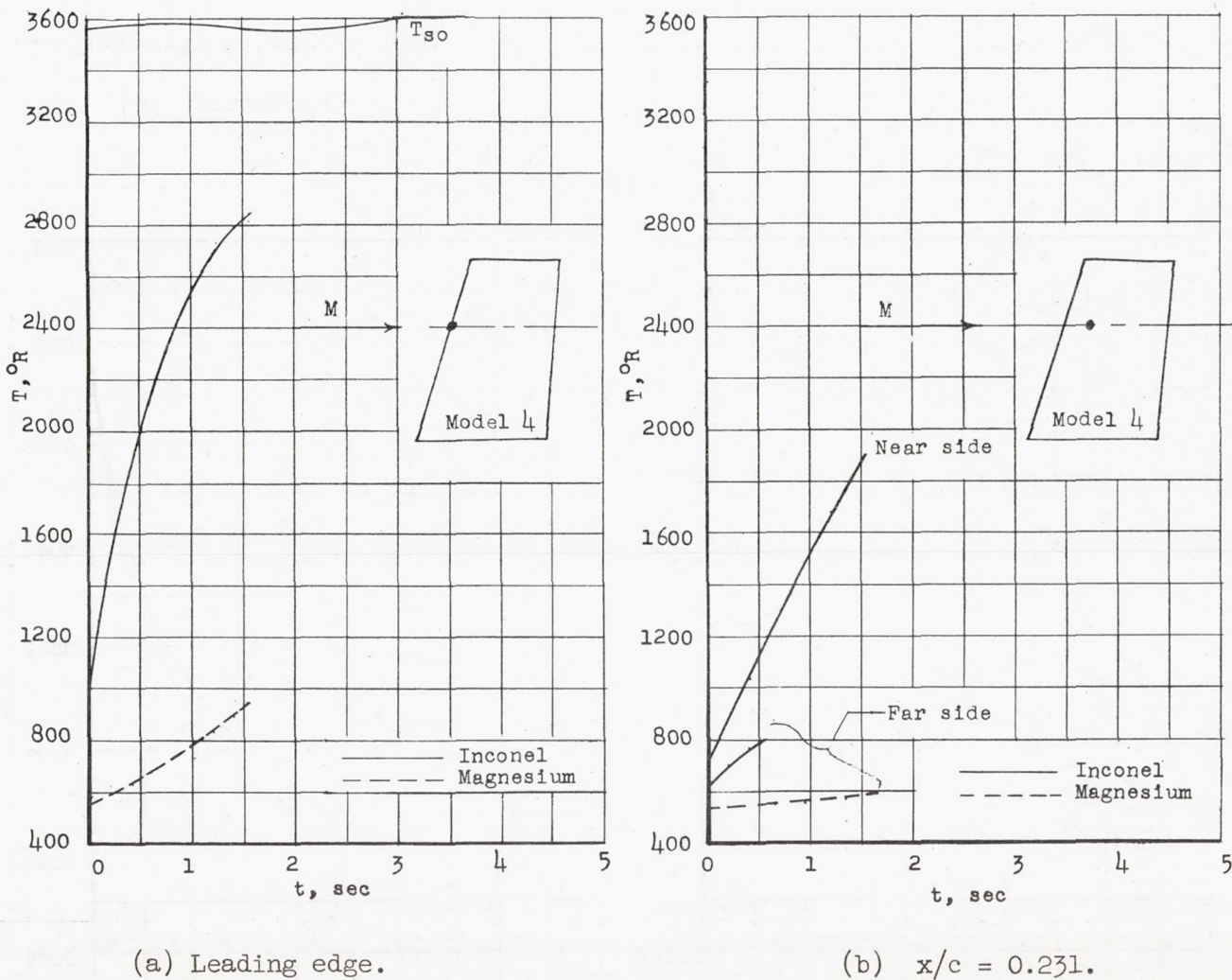


Figure 7.- Temperature time histories obtained during test of model 4. Free oxygen in stream about 6.9 percent by volume.

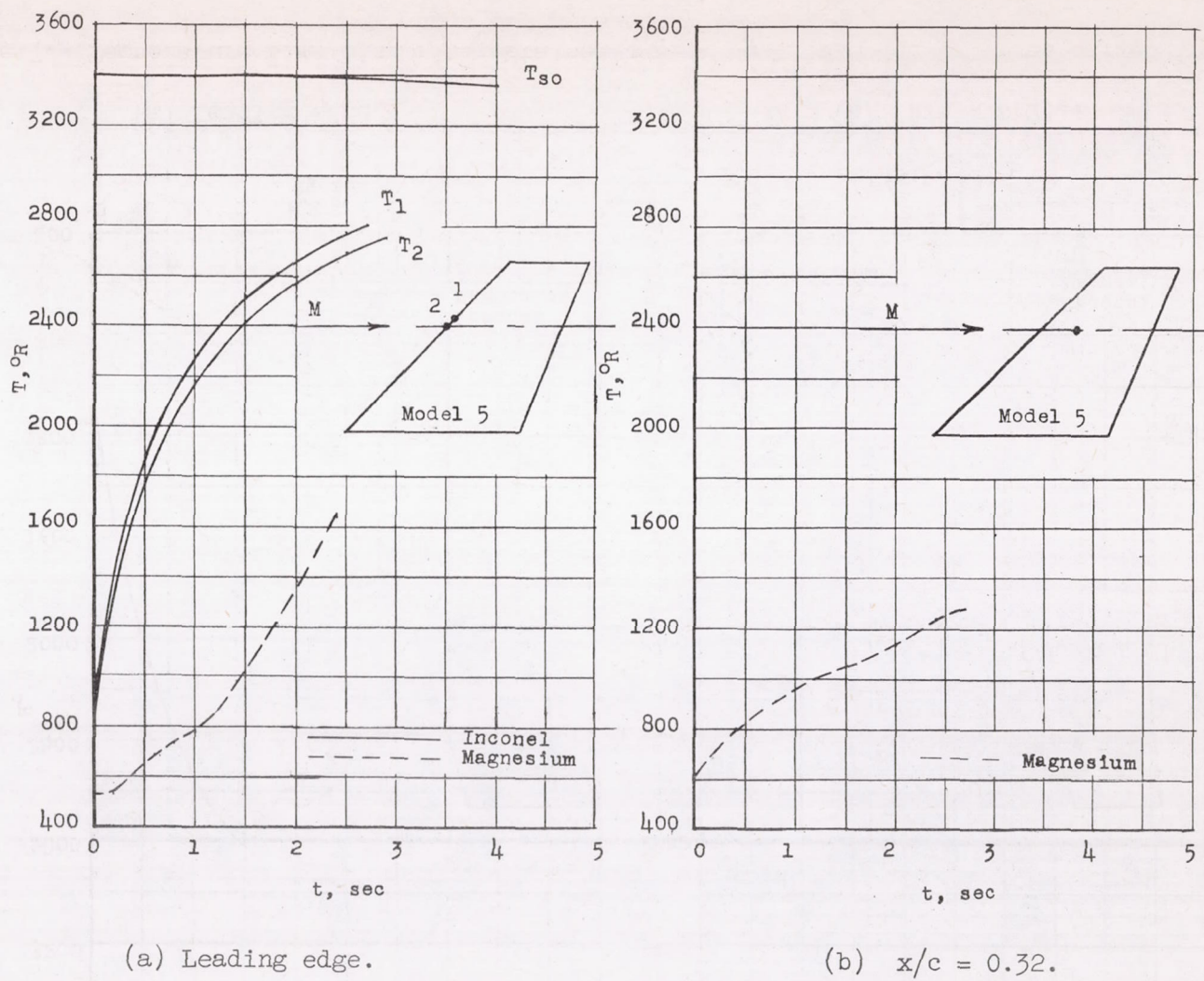


Figure 8.- Temperature time histories obtained during test of model 5. Free oxygen in stream about 7.9 percent by volume.

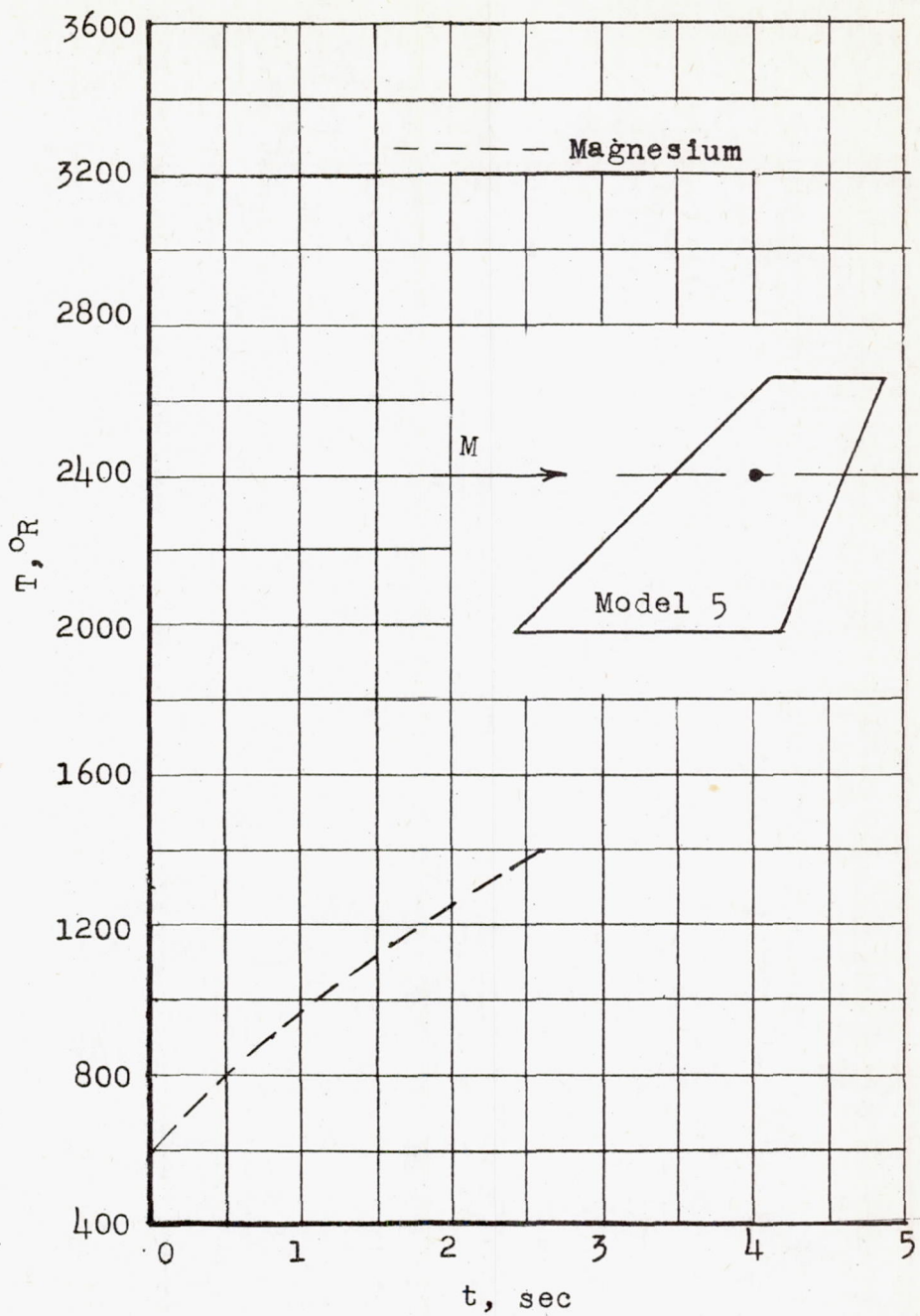
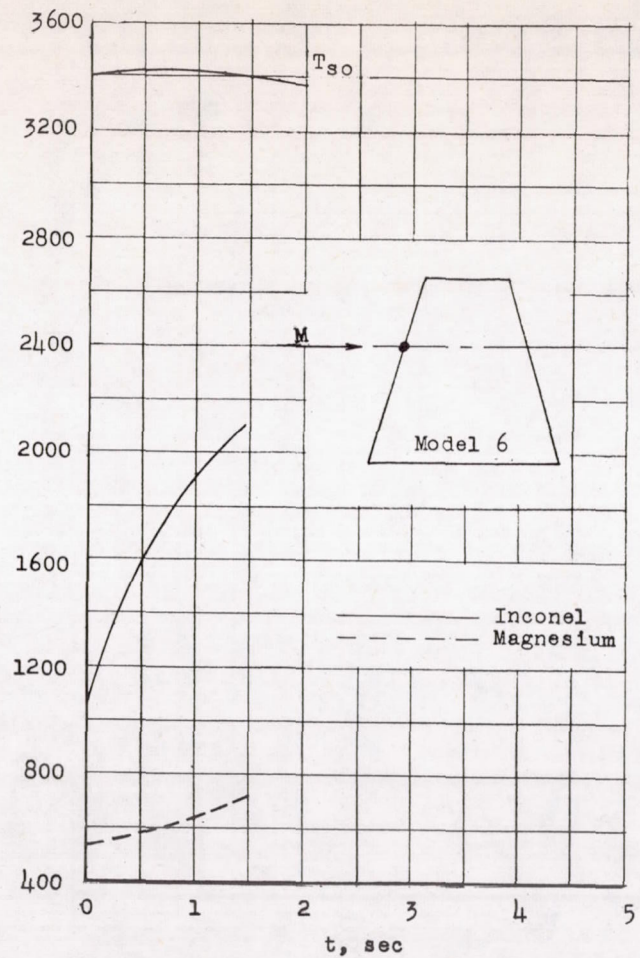
(c) $x/c = 0.50.$

Figure 8.- Concluded.



(a) Leading edge.

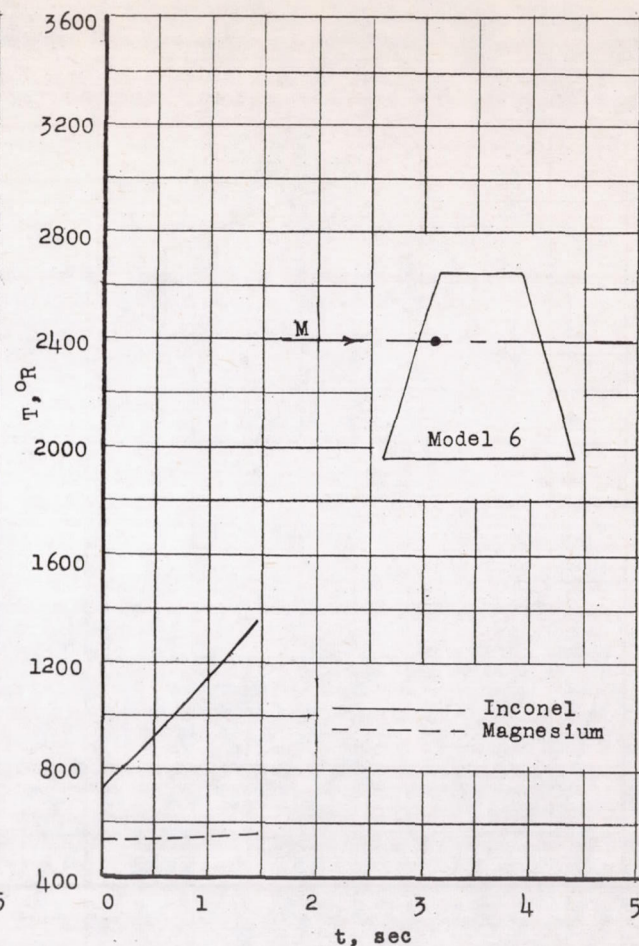
(b) $x/c = 0.133$.

Figure 9.- Temperature time histories obtained during test of model 6. Free oxygen in stream about 7.8 percent by volume.

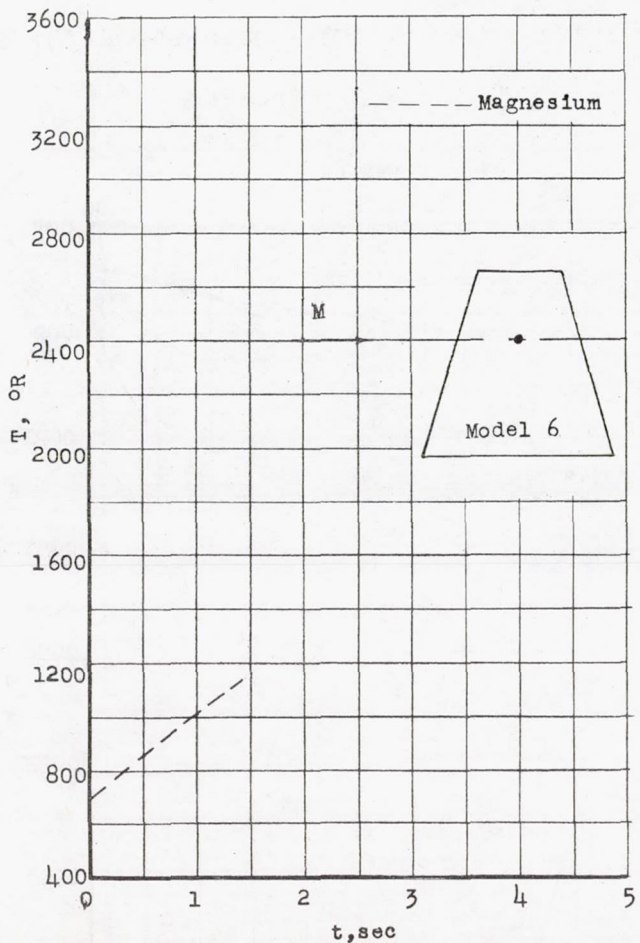
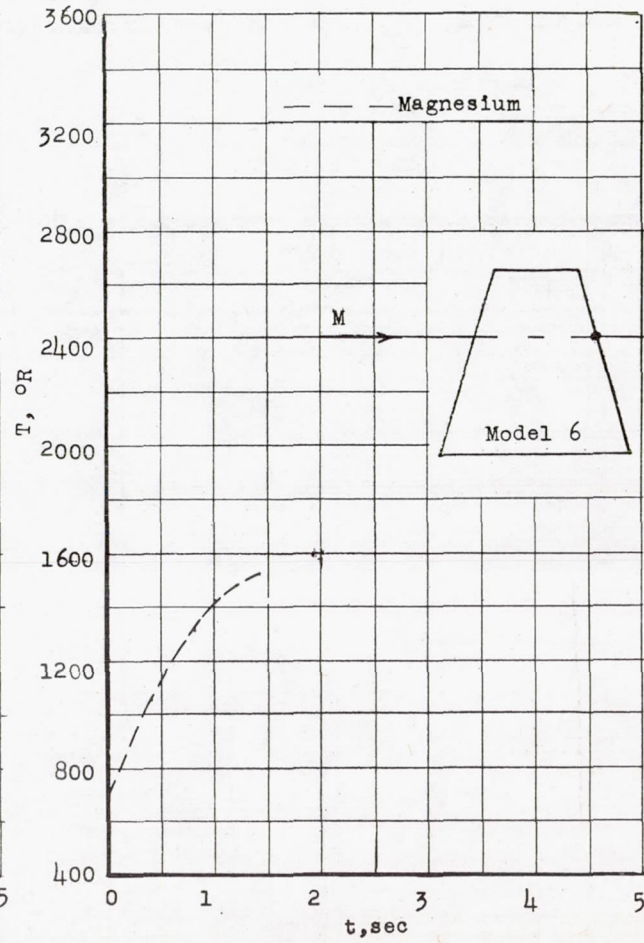
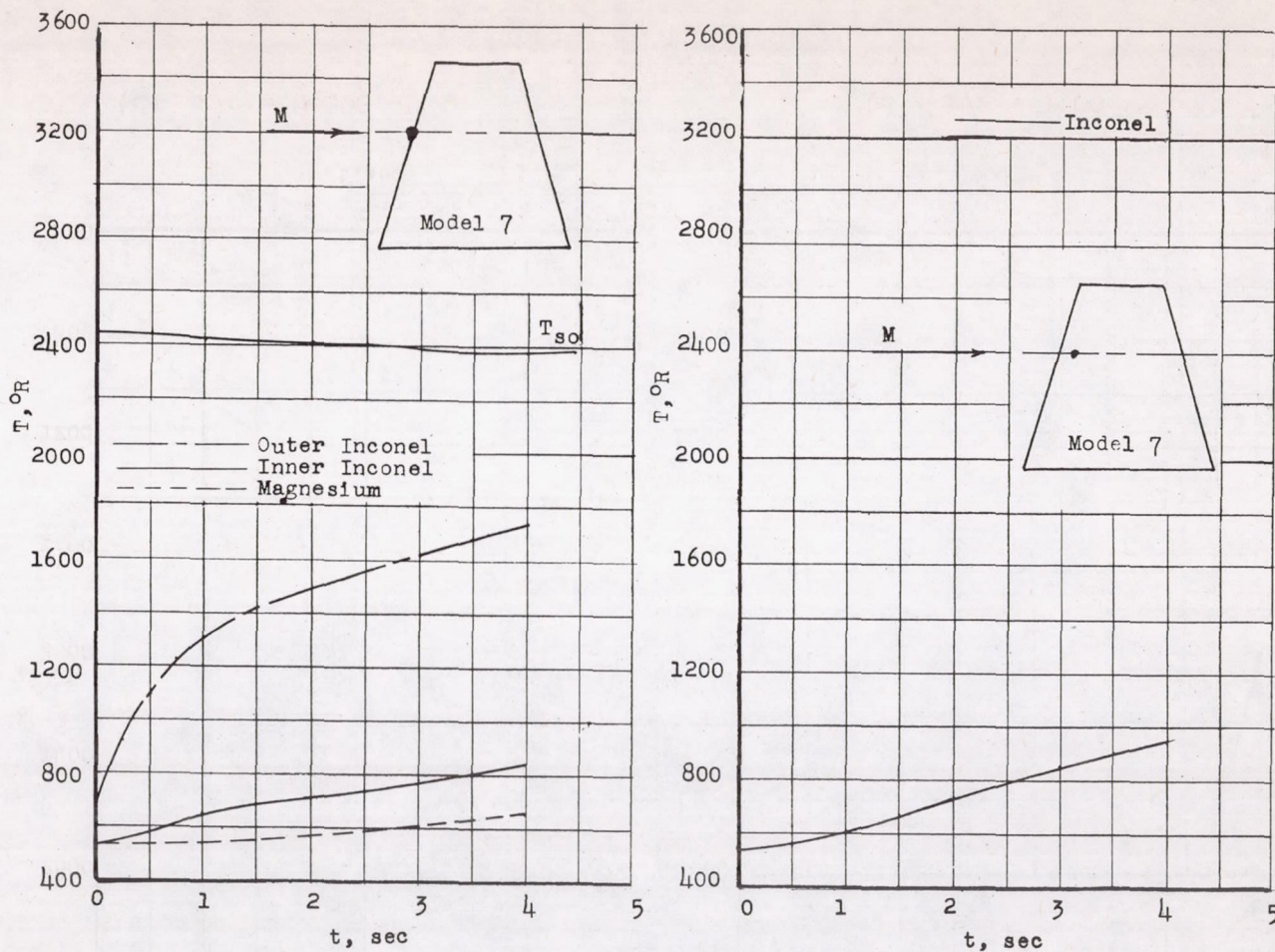
(c) $x/c = 0.500.$ (d) $x/c = 1.00.$

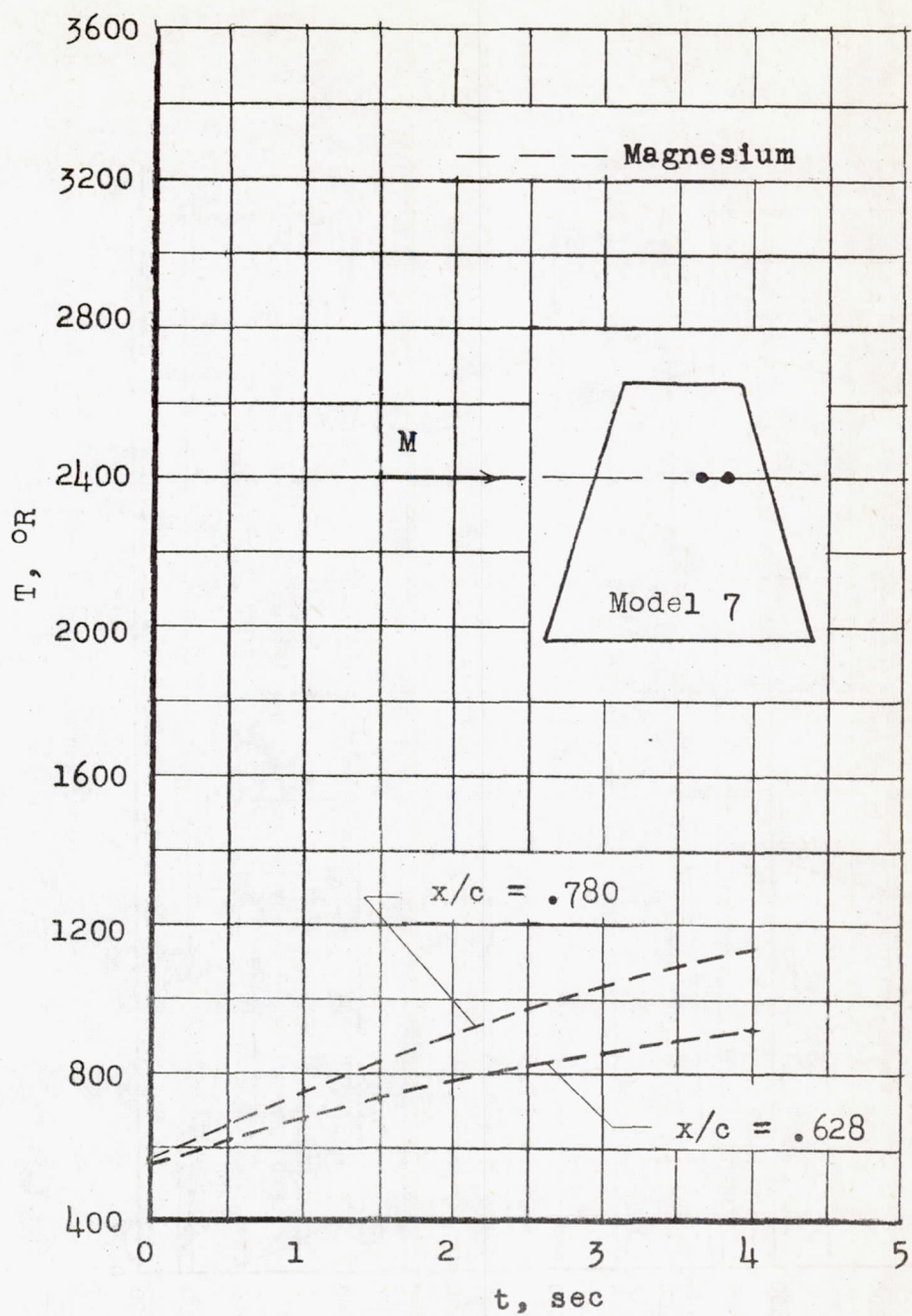
Figure 9.- Concluded.



(a) Leading edge.

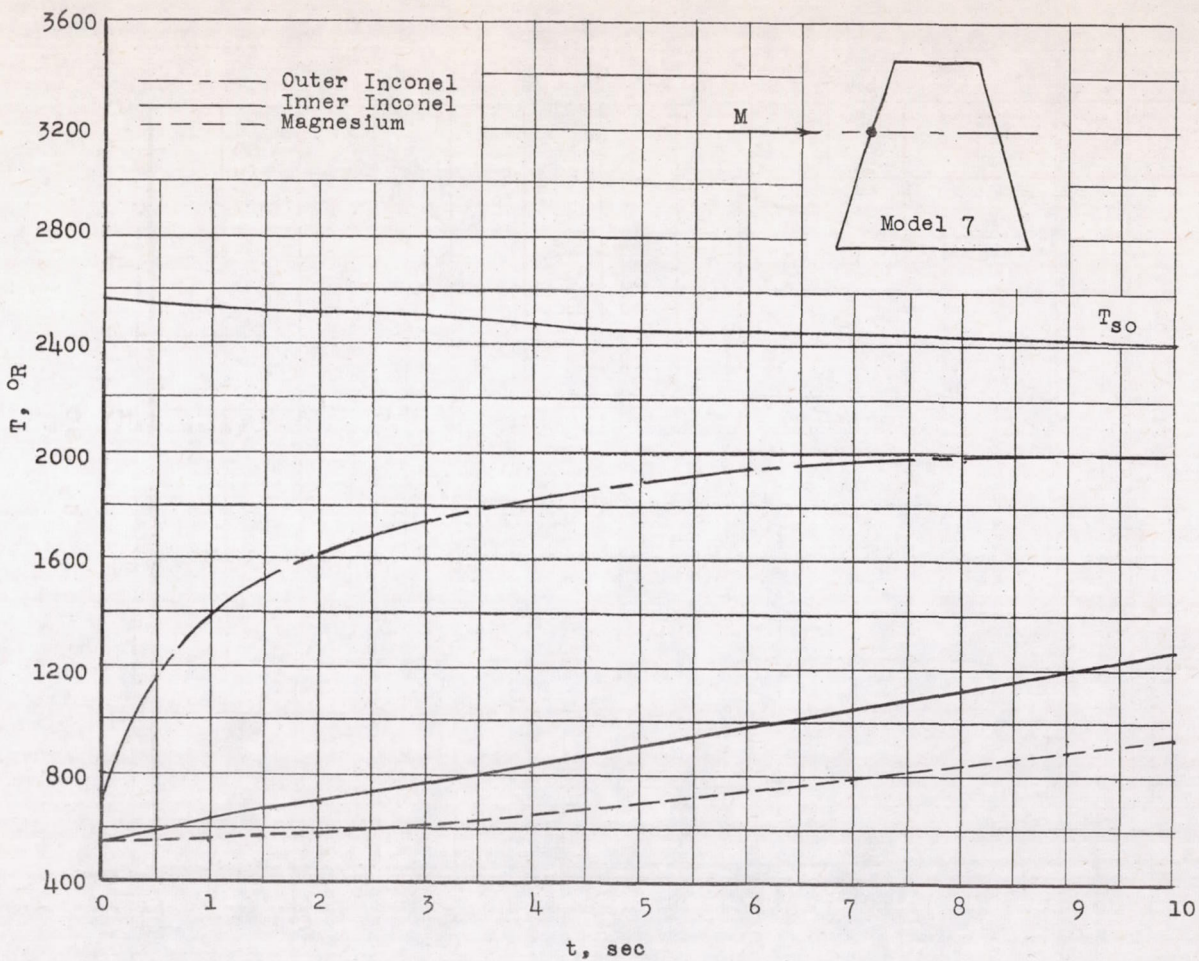
(b) $x/c = 0.147$.

Figure 10.- Temperature time histories obtained during test of model 7. Free oxygen in stream about 13.0 percent by volume.



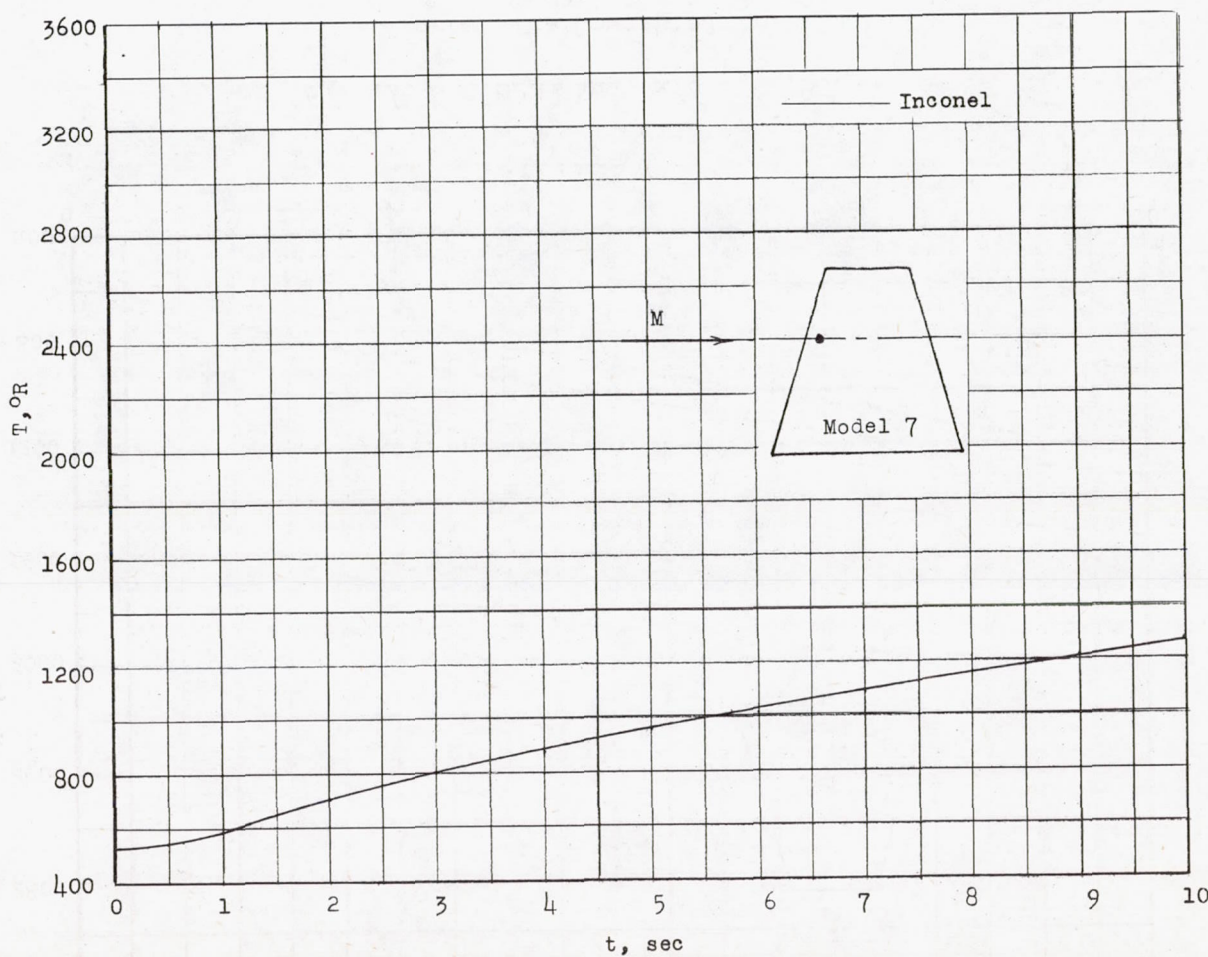
(c) $x/c = 0.628; x/c = 0.780.$

Figure 10.- Concluded.



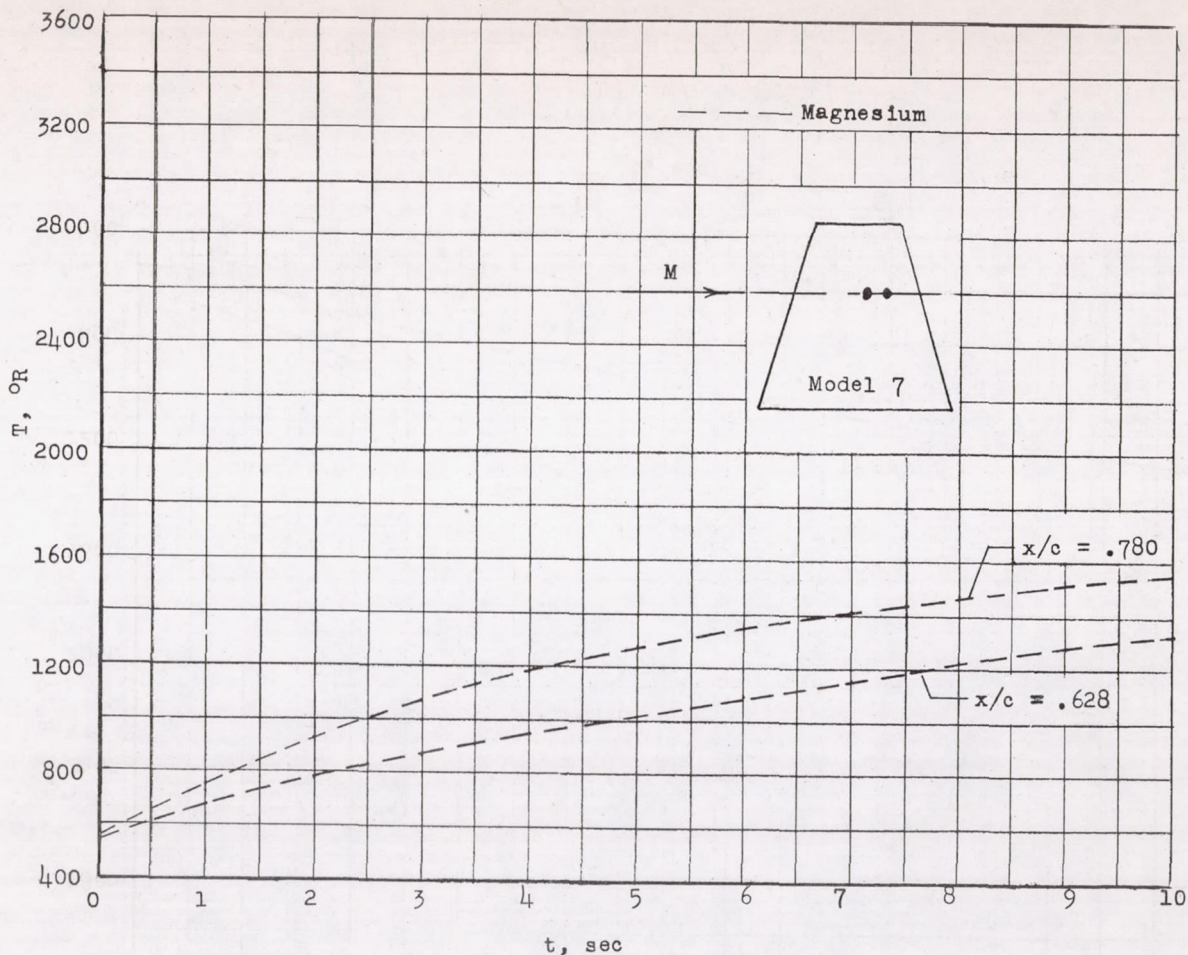
(a) Leading edge.

Figure 11.- Temperature time histories obtained during test of model 7. Free oxygen in stream about 12.6 percent by volume.



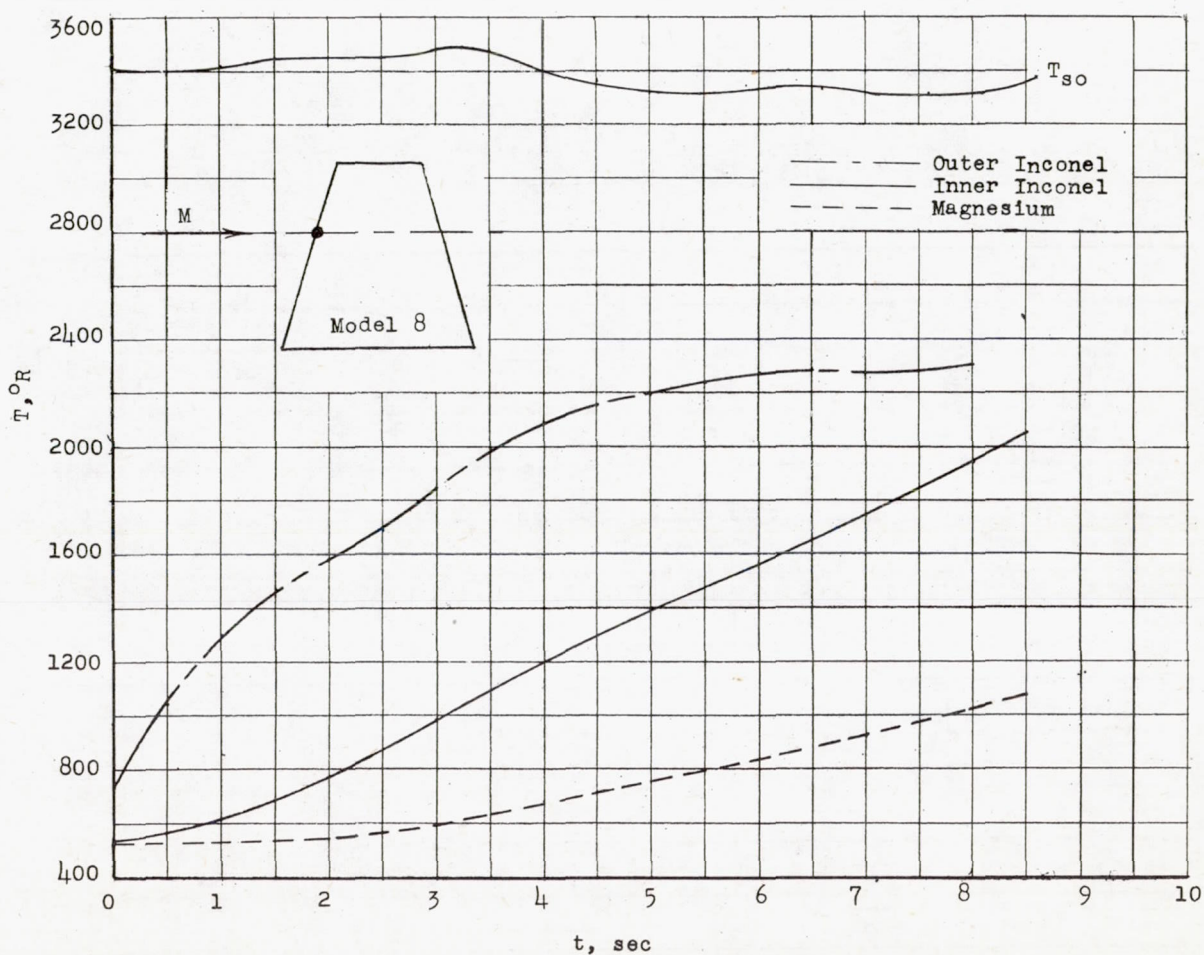
(b) $x/c = 0.147$.

Figure 11.- Continued.



(c) $x/c = 0.628$ and $x/c = 0.780.$

Figure 11.- Concluded.



(a) Leading edge.

Figure 12.- Temperature time histories obtained during test of model 8. Free oxygen in stream about 7.8 percent by volume.

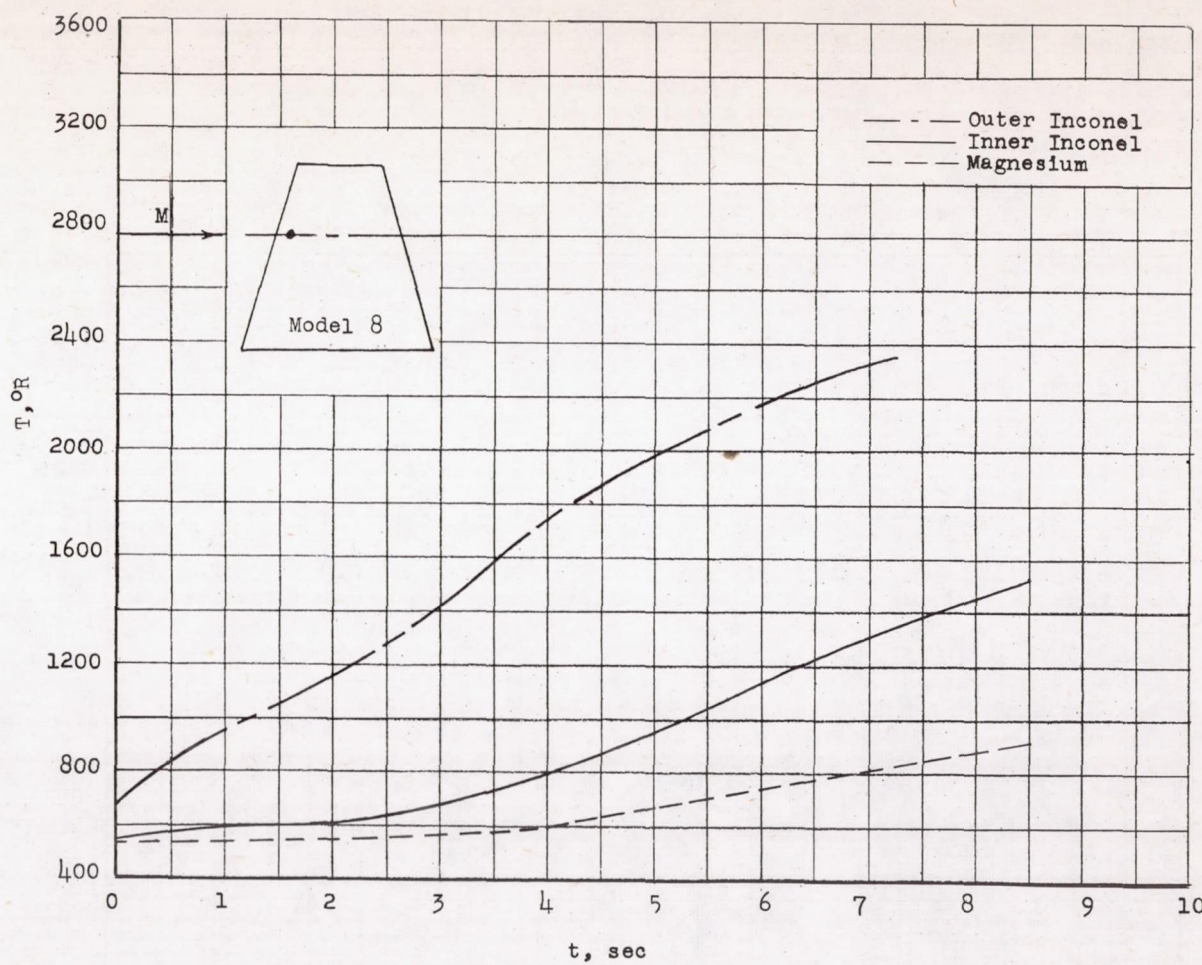
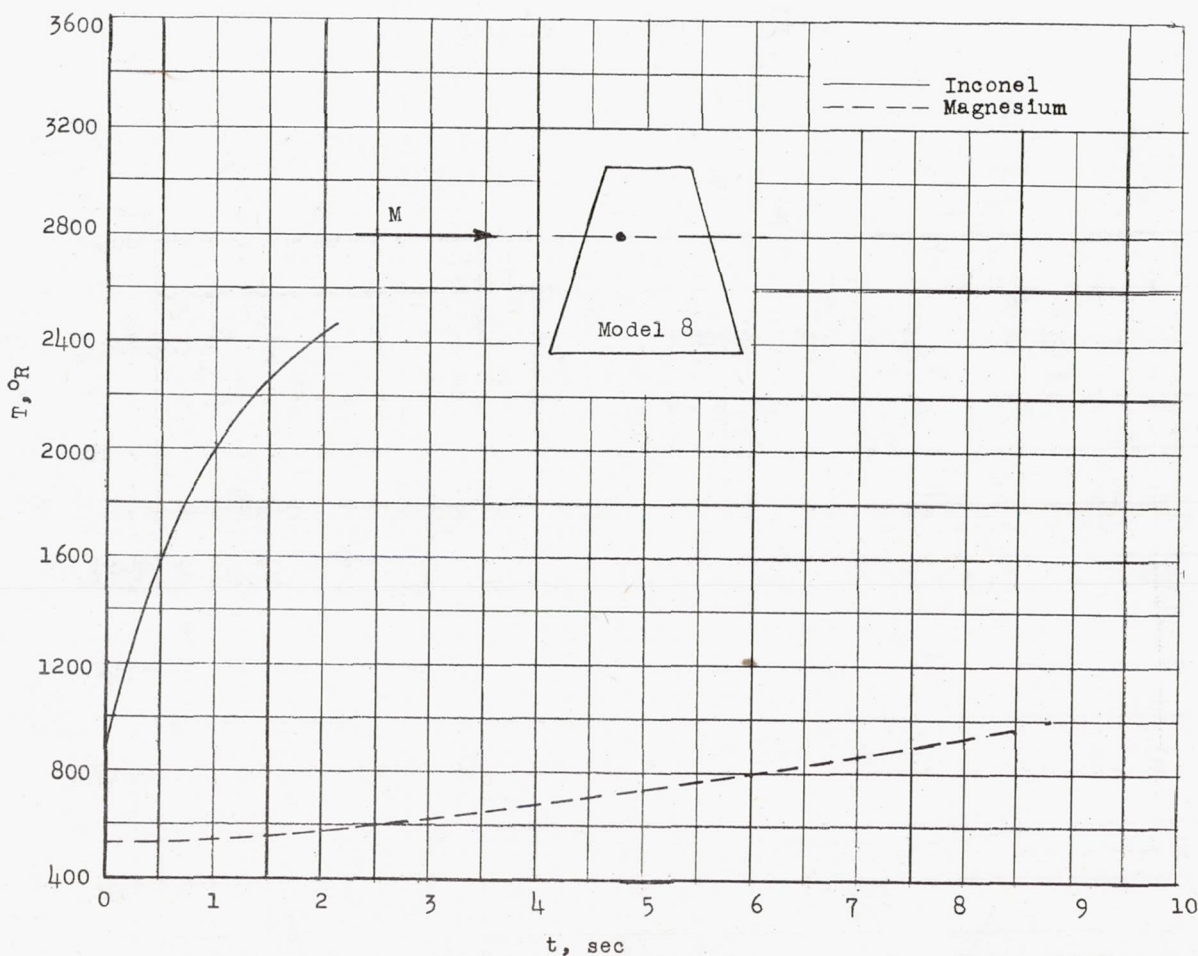
(b) $x/c = 0.133.$

Figure 12.- Continued.



(c) $x/c = 0.266$.

Figure 12.- Continued.

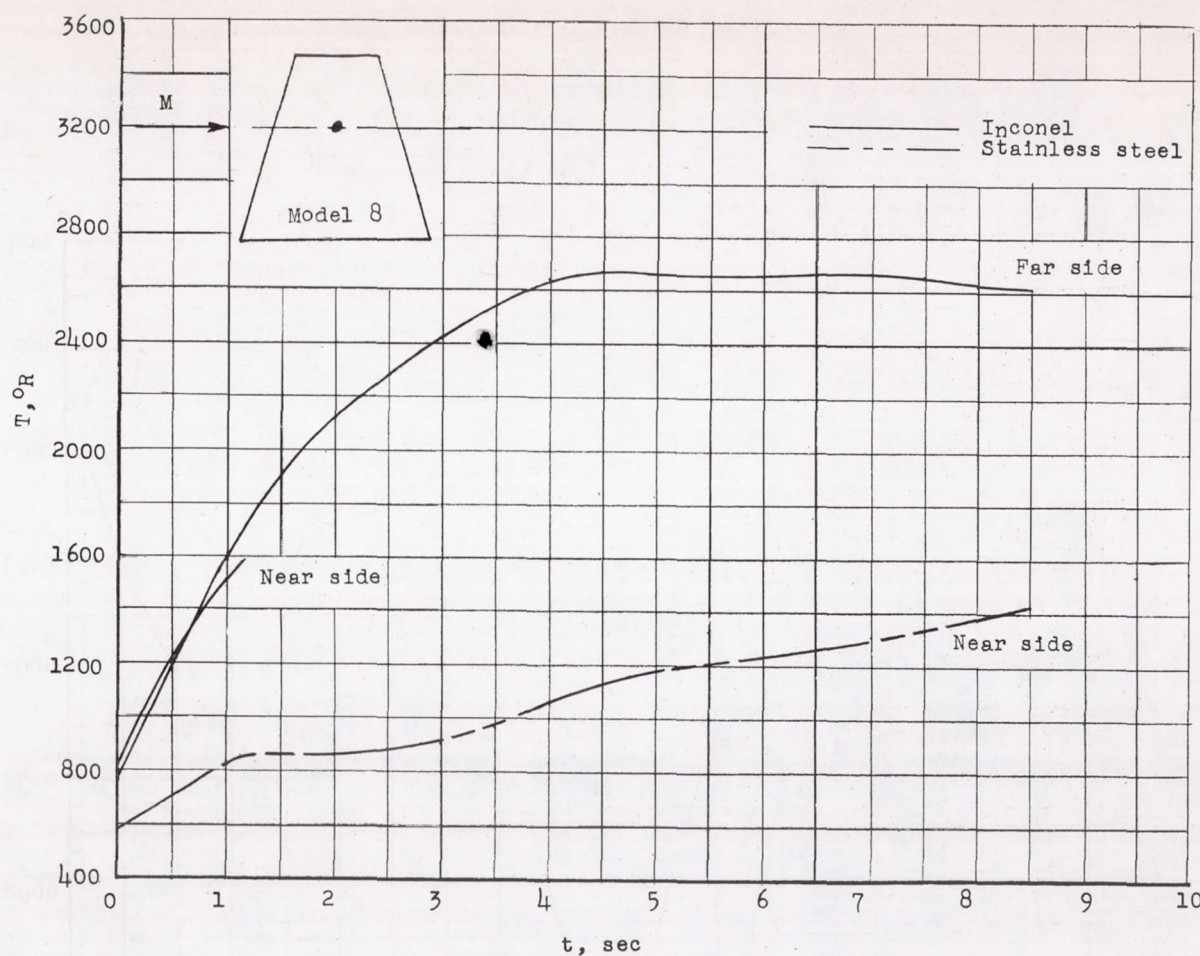
(d) $x/c = 0.50.$

Figure 12.- Continued.

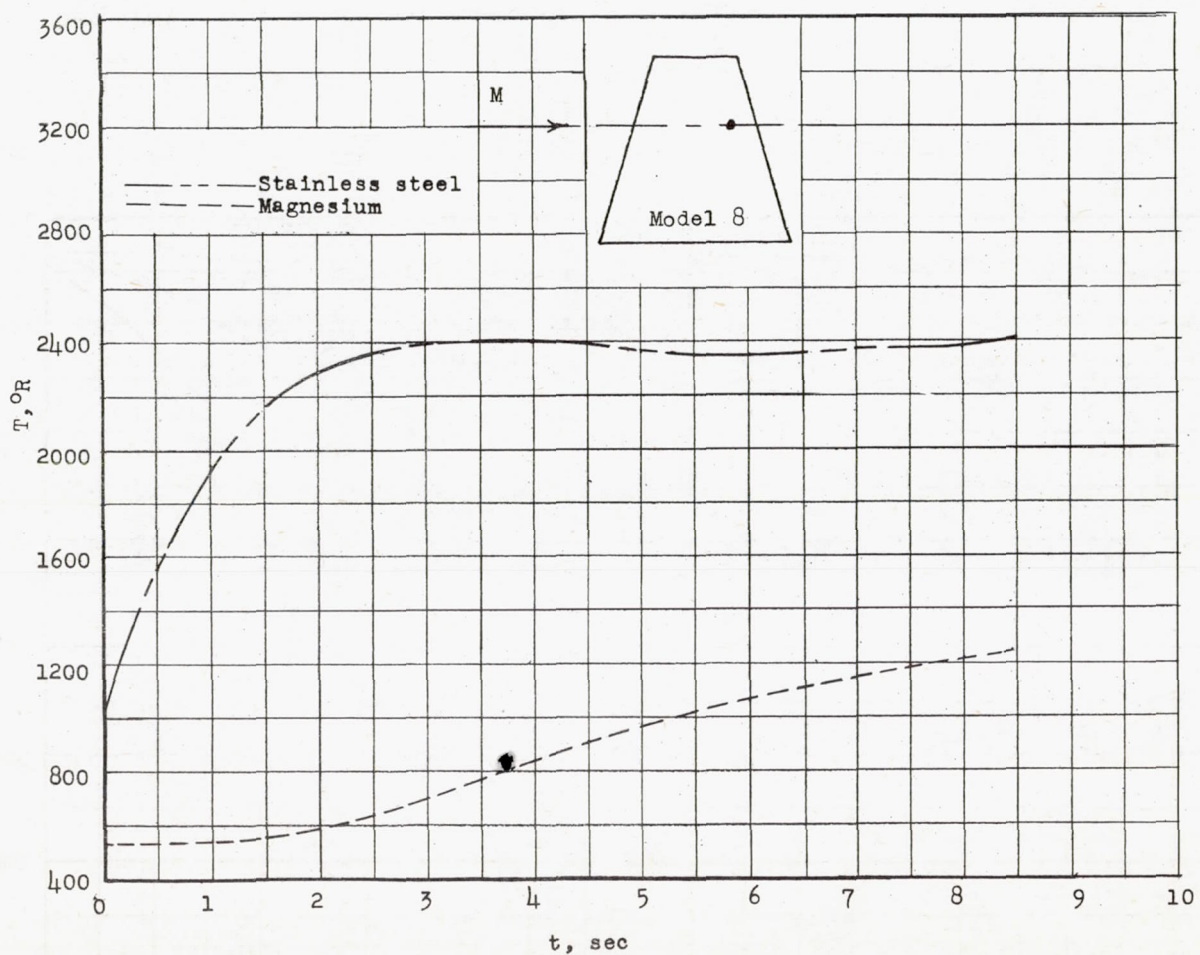
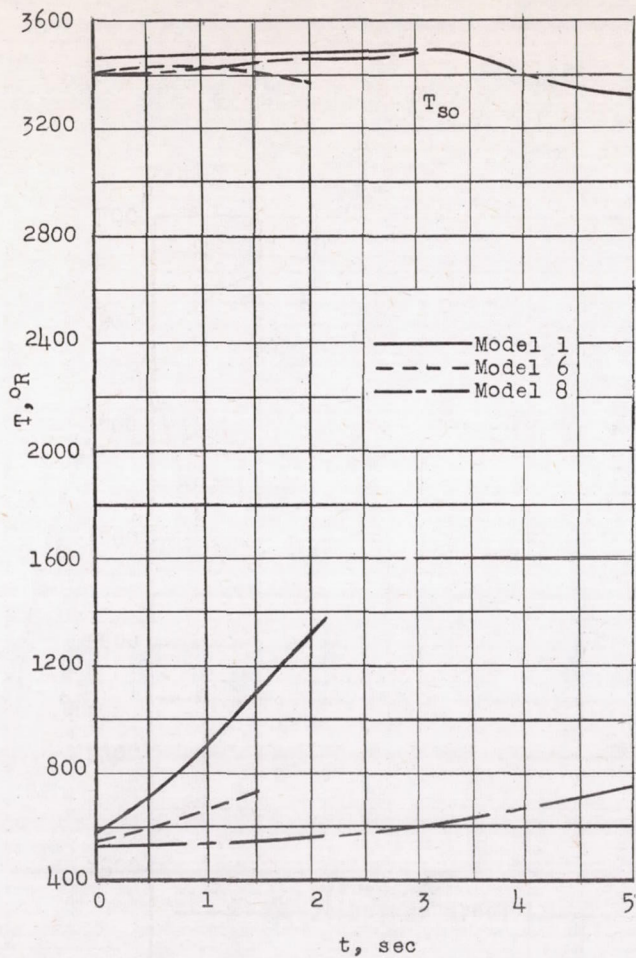
(e) $x/c = 0.75.$

Figure 12.- Concluded.



(a) Leading edge.

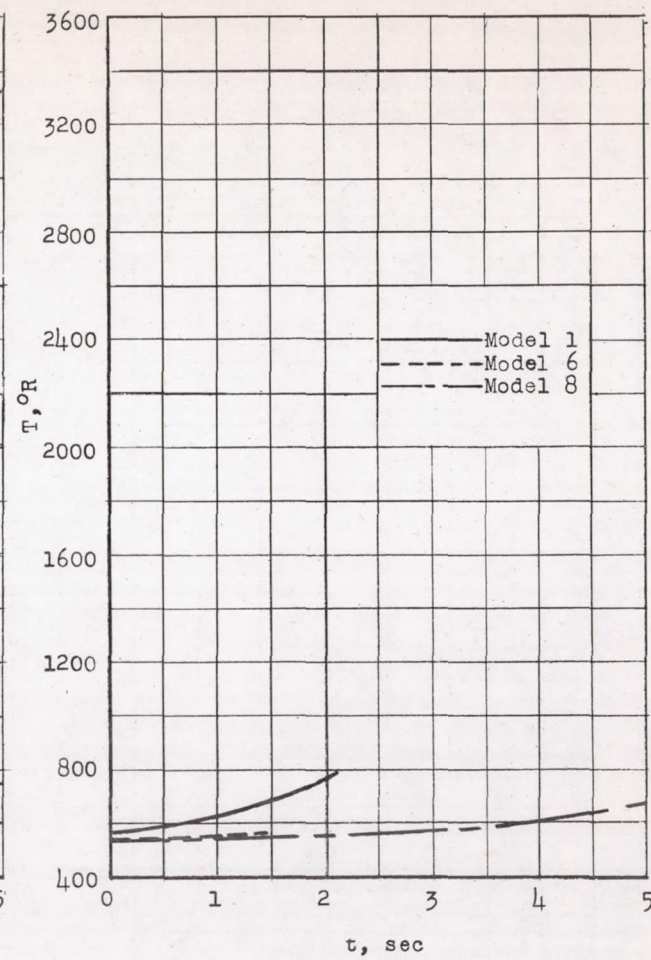
(b) $x/c = 0.133$.

Figure 13.- Temperatures measured in magnesium with simple leading-edge protection of model 1, modified simple leading-edge protection of model 6, and more complete protection of model 8.

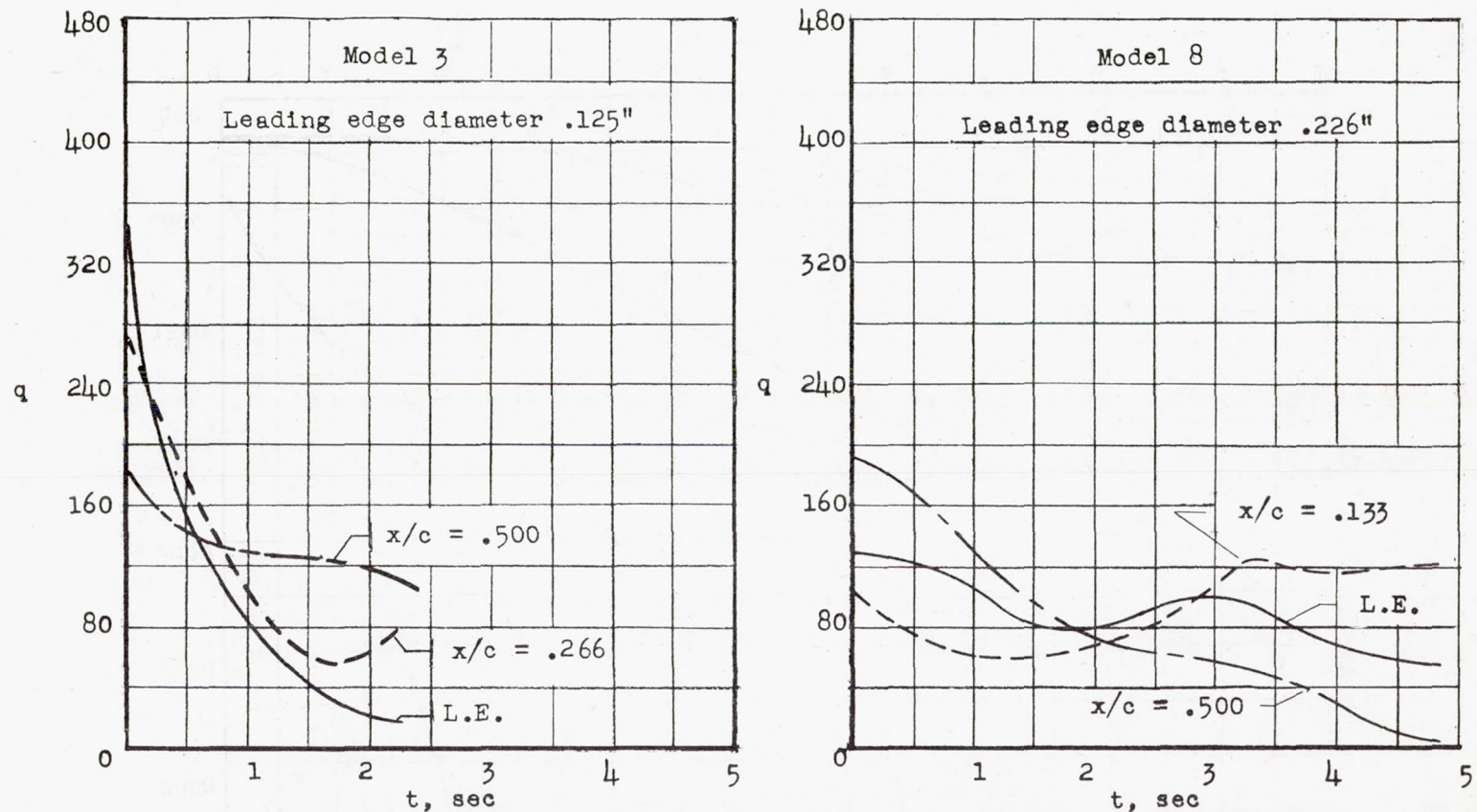


Figure 14.- Variation of total heat flux with time at several stations on models 3 and 8 as calculated from measured temperatures in different layers of material.

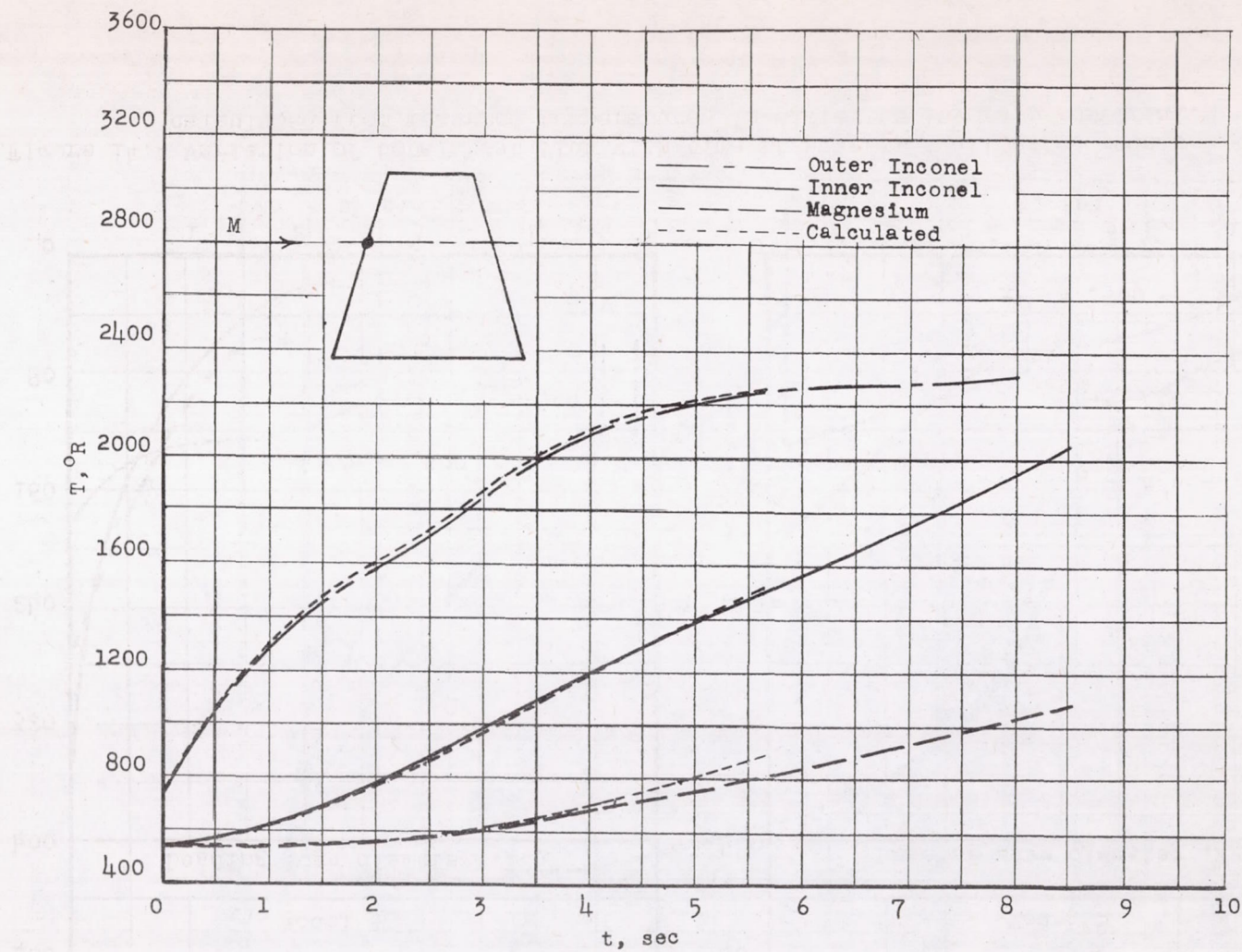


Figure 15.- Comparison between measured temperatures and those calculated with simple heat-balance relations with an effective gap of 0.0035 inch between outer layers and an effective gap of 0.0100 inch between inner layer of Inconel and magnesium at leading edge of model 8.

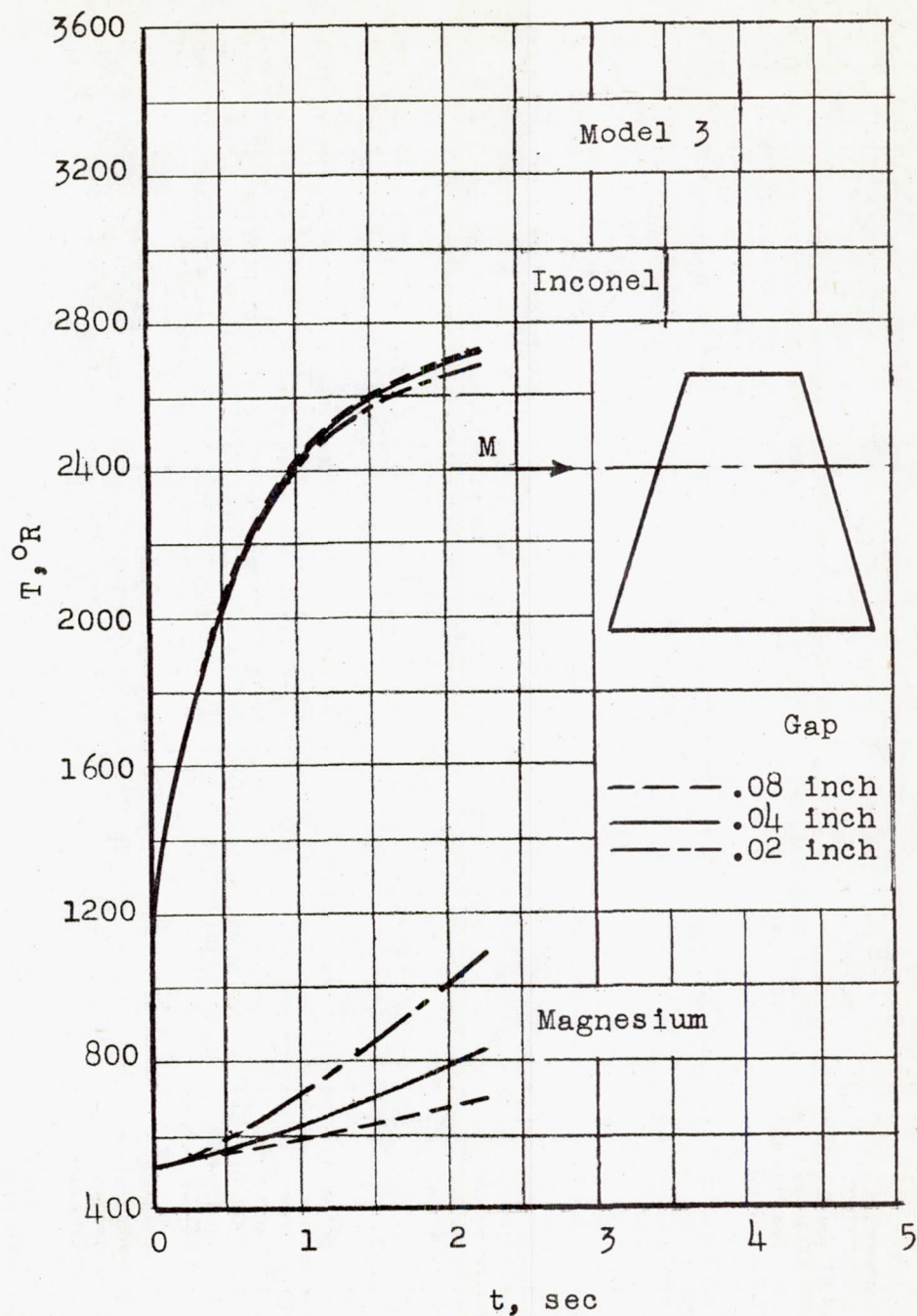


Figure 16.- Comparison between temperatures calculated with simple heat-balance relations to show effect of gap magnitude.